

Geodesic Distance in Planar Graphs: An Integrable Approach

P. Di Francesco¹

Service de Physique Théorique, CEA/DSM/SPhT

Unité de recherche associée au CNRS

CEA/Saclay

91191 Gif sur Yvette Cedex, France

We discuss the enumeration of planar graphs using bijections with suitably decorated trees, which allow for keeping track of the geodesic distances between faces of the graph. The corresponding generating functions obey non-linear recursion relations on the geodesic distance. These are solved by use of stationary multi-soliton tau-functions of suitable reductions of the KP hierarchy. We obtain a unified formulation of the (multi-) critical continuum limit describing large graphs with marked points at large geodesic distances, and obtain integrable differential equations for the corresponding scaling functions. This provides a continuum formulation of two-dimensional quantum gravity, in terms of the geodesic distance.

10/03

¹ philippe@spht.saclay.cea.fr

1. Introduction

The work presented in this note was initially motivated by the need to better understand on a combinatorial level the various results obtained via matrix models on the enumeration of graphs with fixed topology [1] (see also [2] and [3] and references therein). The early work on this subject dates back to a combinatorist, W. Tutte [4], who managed to enumerate many of the planar versions of these using recursion relations in the spirit of what we call today “loop equations” for matrix models. Such an approach, though combinatorial, failed to really explain the simplicity of the algebraic equations determining the generating functions for planar graphs. Another motivation comes from the physics of two-dimensional quantum gravity. At the discrete level, coupling matter to gravity simply amounts to define a statistical model (typically with local Boltzmann weights) on a fluctuating base space, in the form of random discretized surfaces. The continuum version of this involves field-theoretical descriptions of random surfaces with critical matter [5], via the coupling of conformal field theories (matter) to the Liouville field theory (metrics of the underlying space).

The interpretation of the planar graph results remained elusive until the groundbreaking work of G. Schaeffer [6], who finally gave a beautifully simple combinatorial explanation for these algebraic equations, in terms of decorated trees. The idea was simply to establish bijections between classes of planar graphs and suitably decorated trees, then easily enumerated via algebraic relations obeyed by their generating functions. This technique proved quite general, and was extended to many classes of planar graphs, including graphs of arbitrary valence [7], special classes of bipartite graphs called constellations [8] [9] and other classes of bipartite graphs [10], including the particular cases of hard objects on planar graphs [11] and of the Ising model on planar graphs [12].

The great advantage of this bijective enumeration is that it allows for keeping track of some details of the graphs in the language of trees. An important example of this concerns the geodesic distance between say the vertices of random quadrangulations, namely planar graphs with only tetravalent faces. In [13], it was shown that the geodesic distance of all vertices from an origin vertex of the graph may translate into integer vertex labels in some corresponding trees, themselves realizing a discrete version of the Brownian snake, further studied and extended in [14] in the language of spatial branching processes. In [15], it was shown that the generating functions for planar graphs with two external legs obeyed non-linear recursion relations on the maximal geodesic distance between the legs, and it is the purpose of this note to clarify and extend the results of this paper.

Note that no continuum (field-theoretical) treatment of two-dimensional quantum gravity in terms of geodesic distance is available yet, only some partial results were obtained using a transfer matrix formalism [16] [17] [18] leading to some conjectural continuum expression for a scaling function of the geodesic distance in the case of pure gravity without matter. The present work provides an alternative solution and gives access to a host of scaling functions for various (multi-) critical models of matter systems coupled to two-dimensional quantum gravity.

The paper is organized as follows. In Sects. 2,3 and 4, we recall some known facts on the bijective enumeration of planar graphs with respectively even valences, arbitrary (even and odd) valences, and bicolored vertices. This relies on an iterative cutting procedure which, starting from a planar graph, produces a decorated rooted tree. In turn the tree may be closed back in a unique way into a planar graph, and we use this bijection to recover the algebraic relations satisfied by the various counting functions involved. Sect. 5 is devoted to the introduction of the geodesic distance in the various enumeration problems at hand: we present a unified picture involving formal operators Q generating the descendent trees around a vertex, and allowing for keeping track of the geodesic distance from the root to the external face of the planar graph to which the tree closes back. The main results are recursion relations on the geodesic distance satisfied by the generating functions for planar graphs with legs. In Sect. 6, we solve exactly a number of these recursion relations, by expanding the generating functions at large maximal geodesic distance n , and resumming the resulting series. These display a remarkable “integrable” structure in that they generically involve tau-functions of the KP hierarchy. Sect. 7 is devoted to the critical continuum limit of the problem, in which we consider large planar graphs and large geodesic distances. The generating functions calculated in Sect. 6 are shown to yield universal scaling functions, characteristic of the various (multi-) critical points of random surfaces with matter and with marked points at a fixed geodesic distance. We propose a generalization of our results based on differential equations obeyed by the scaling functions, and illustrate it in the case of the Ising model on random surfaces. Finally, we gather a few concluding remarks in Sect. 8, where in particular we discuss the integrable structure of our recursion relations, and of their continuum counterparts.

2. Planar graphs and trees I: the case of even valences

In this section, we recall some results on the enumeration of planar graphs of even valence with two extra “legs”. This is done via a bijection between planar graphs and decorated trees, easily enumerated.

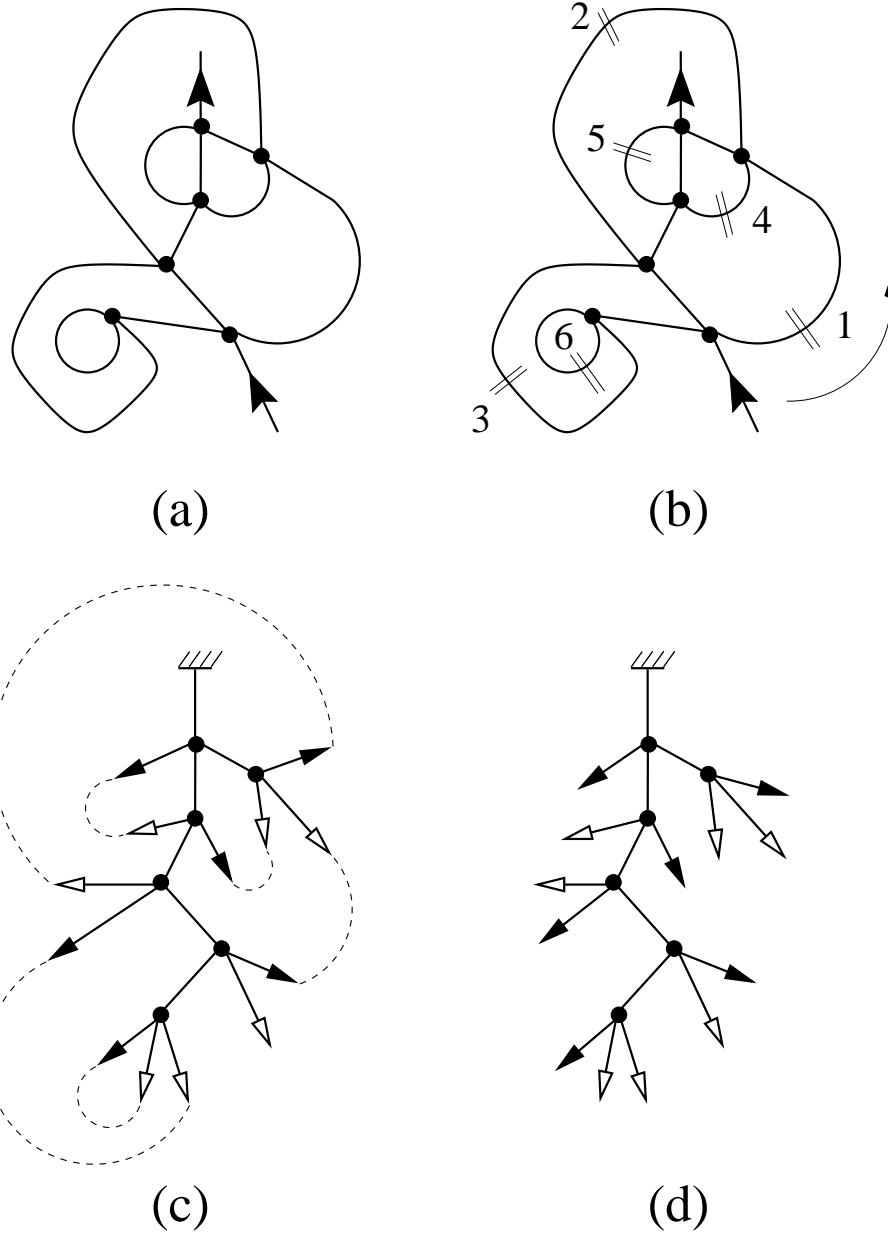


Fig.1: The bijection between planar tetravalent graphs with two legs (a) and rooted ternary blossom-trees (d) is obtained via the following cutting procedure. We first visit all edges of the graph in counterclockwise direction (b) and cut them iff the resulting graph is still connected: we have indicated the succession of cut edges by their number in the order of visit, from 1 to 6 here. The cut edges are then replaced by pairs of white and black leaves (c). Moreover the incoming leg is replaced by a white leaf and the outgoing one by a root, finally yielding a rooted ternary blossom-tree (d).

2.1. *Tetravalent graphs*

We wish to compute the generating function $R \equiv R(g)$ for planar tetravalent graphs

with two distinguished (say in- and out-coming) univalent vertices, and with a weight g per tetravalent vertex. These will be referred to as “two-leg diagrams” in the following, the legs denoting simply the edges connecting the two univalent vertices to the graph. For definiteness, we will always represent these planar graphs with the incoming leg adjacent to the external face. Note that the outgoing one need not be adjacent to the same face, as in the example of Fig.1 (a).

The computation of R relies on the following bijection, illustrated in Fig.1, between two-leg diagrams and so-called rooted blossom-trees [7]. Starting from a two-leg diagram (Fig.1 (a)), let us first visit all edges adjacent to the external face, starting from the incoming leg and in counterclockwise order. Successively, each visited edge is cut iff the cut diagram remains connected (Fig.1 (b)). The cut ends of the edge are then decorated respectively with a black and a white leaf. Once all edges adjacent to the external face have been visited, we repeat the procedure with the newly cut diagram. The process ends when all faces of the original diagram have been merged with the external one. The resulting graph is nothing but a planar tree (it has only one face), with black and white leaves (Fig.1 (c)). Note that by construction there is exactly one black leaf connected to each internal vertex of the tree. Finally, we replace the incoming vertex by a white leaf and the outgoing one by a root, so that there is exactly one more white leaf than black ones (Fig.1 (d)). We define rooted blossom-trees as planar rooted ternary trees with black and white leaves, and such that there is exactly one black leaf at each internal vertex. Our cutting procedure has produced a rooted blossom-tree out of any two-leg diagram. The process however is readily seen to be invertible as there is a unique way of re-connecting the black-white leaf pairs into edges, by connecting each black leaf to the first available white leaf in counterclockwise order around the tree (the dashed lines of Fig.1 (c)). This establishes the desired bijection between the two objects.

Counting rooted blossom-trees is now an easy task, performed for instance by inspection of all possible environments of the vertex connected to the root. This leads straightforwardly to the relation

$$R = 1 + 3gR^2 \tag{2.1}$$

where the first term 1 counts the possibility that the root be directly connected to a leaf, and the second term accounts for the three possible positions for the black leaf around this vertex, itself receiving the weight g , while the two other descendents of the vertex are themselves rooted blossom-trees. From its very definition as counting function, R admits a power series expansion in g , with $R = 1 + O(g)$. This fixes it uniquely to be

$$R = \frac{1 - \sqrt{1 - 12g}}{6g} \quad (2.2)$$

The series for R has a finite convergence radius $g_c = 1/12$. When g approaches g_c (critical limit), the contribution of large graphs becomes dominant, and we learn that the number of graphs with N vertices behaves as $g_c^{-N}/N^{3/2}$ for large N .

Note that $R(g) = C(3g)$ where C denotes the generating function for Catalan numbers $c_N = \binom{2N}{N}/(N+1)$, which count among other things the rooted planar binary trees with N inner vertices, with the convention that $c_0 = 1$. The number of rooted blossom trees with N inner vertices is obtained by considering rooted planar binary trees with all leaves white and by decorating each vertex with a black leaf: it reads therefore $3^N c_N$ as there are three choices for the position of the black leaf at each inner vertex.

2.2. General case of graphs with even valences

The bijection of previous section may be extended to include two-leg-diagrams of graphs with arbitrary even valences $v = 4, 6, 8, \dots$. We repeat the exact same cutting procedure and end up with some generalized rooted blossom-trees, such that each inner vertex say of valence $v = 2k$ has exactly $k - 1$ black leaves attached to it. The corresponding generating function $R \equiv R(g_4, g_6, g_8, \dots)$ with say weights g_{2k} per $2k$ -valent vertex, $k = 2, 3, 4, \dots$ obeys the following relation

$$R = 1 + \sum_{k \geq 2} g_{2k} \binom{2k-1}{k} R^k \quad (2.3)$$

obtained again by inspecting all possible environments of the vertex attached to the root. The combinatorial factor $\binom{2k-1}{k}$ accounts for the number of choices for the positions of the $k - 1$ black leaves around the vertex, while the remaining k descendents are themselves rooted blossom-trees.

Again, R is the unique solution to (2.3) that admits a power series expansion in the g_{2i} 's, with $R = 1 + O(g_{2i})$ for all $i \geq 2$.

3. Planar graphs and trees II: arbitrary valences

This section extends the results of the previous one to graphs with both even and odd valences. The first consequence of allowing for odd valences is the existence of one-leg diagrams with only one (outcoming) external leg. These will be represented in the plane like two-leg diagrams, but the leg need not be adjacent to the external face.

3.1. Trivalent graphs

Let $S \equiv S(g)$ and $R \equiv R(g)$ denote the generating functions for respectively one- and two-leg diagrams of trivalent planar graphs, with a weight g per trivalent vertex. Applying the cutting procedure of previous sections to one and two-leg diagrams, we end up with two types of rooted blossom trees which we call S-trees and R-trees respectively. Note that the unique (outcoming) leg of the one-leg diagrams is replaced by a root in the corresponding blossom-tree. To characterize S- and R-trees, let us introduce the charge q of a tree as its number of white leaves minus that of black ones. For instance, the blossom-trees of Sects. 2.1 and 2.2 above have all charge $q = 1$, the same holds for the present R-trees, while the S-trees are neutral, with charge $q = 0$. Now S-trees and R-trees are characterized among rooted binary blossom-trees as having only descendent subtrees (not reduced to black leaves) of charge 0 or 1, while their total charge is 0 and 1 respectively (this is easily done by following the effect of the cutting procedure on the original graph, see [7] for details). The cutting procedure establishes a bijection between one- and two-leg diagrams and S- and R-trees respectively.

The latter are easily counted, again by inspection of the local environment of the vertex attached to the root. We get the coupled relations:

$$\begin{aligned}
 \begin{array}{c} \text{///} \\ | \\ \textcircled{S} \end{array} &= g \begin{array}{c} \text{///} \\ | \\ \bullet \\ / \quad \backslash \\ \blacktriangleright \quad \textcircled{R} \end{array} + g \begin{array}{c} \text{///} \\ | \\ \bullet \\ \backslash \quad / \\ \textcircled{R} \quad \blacktriangleright \end{array} + g \begin{array}{c} \text{///} \\ | \\ \bullet \\ / \quad \backslash \\ \textcircled{S} \quad \textcircled{S} \end{array} \\
 S &= 2gR + gS^2 \\
 \begin{array}{c} \text{///} \\ | \\ \textcircled{R} \end{array} &= \begin{array}{c} \text{///} \\ | \\ \blacktriangledown \end{array} + g \begin{array}{c} \text{///} \\ | \\ \bullet \\ / \quad \backslash \\ \textcircled{R} \quad \textcircled{S} \end{array} + g \begin{array}{c} \text{///} \\ | \\ \bullet \\ \backslash \quad / \\ \textcircled{S} \quad \textcircled{R} \end{array} \\
 R &= 1 + 2gRS
 \end{aligned} \tag{3.1}$$

respectively displaying contributions from a vertex with total charge 0 (with one black leaf with $q = -1$ and one descendent R-tree with $q = 1$, and two possible positions for the black leaf, or with two descendent S-trees), and from a vertex with total charge 1 (with one descendent S-tree with $q = 0$ and one descendent R-tree with $q = 1$, and two possible relative positions for these).

The generating functions R, S are uniquely determined by the relations (3.1) and the fact that they admit power series expansions $R = 1 + O(g), S = O(g)$.

3.2. General case

The trivalent case is easily extended to the case of arbitrary (even or odd) valences weighted by g_3, g_4, g_5, \dots per tri-, tetra-, penta-,... valent vertex, in which the very same cutting procedure now leads to generalized rooted blossom S- and R-trees, now blossom trees of arbitrary valences $v = 3, 4, 5, \dots$ again further characterized by the fact that all their descendent subtrees not reduced to a black leaf have charge 0 or 1, and by their total charge 0 and 1 respectively. This allows to count them straightforwardly, with the coupled relations:

$$\begin{aligned} S &= \sum_{k \geq 3} g_k \sum_{j=0}^{\lfloor \frac{k-1}{2} \rfloor} \binom{k-1}{j} \binom{k-1-j}{j} R^j S^{k-1-2j} \\ R &= 1 + \sum_{k \geq 3} g_k \sum_{j=0}^{\lfloor \frac{k-2}{2} \rfloor} \binom{k-1}{j} \binom{k-1-j}{j+1} R^{j+1} S^{k-2-2j} \end{aligned} \tag{3.2}$$

where the combinatorial factors account for the possible ways of positioning j black leaves, j or $j+1$ descendent R-subtrees and the remaining S-subtrees on the vertex attached to the root. Again, eqs.(3.2) determine completely R and S with $R = 1 + O(g_i)$ and $S = O(g_i)$ for all $i \geq 3$.

For illustration, in the case of tri/tetravalent graphs, where only g_3, g_4 are non-zero, we have the equations

$$\begin{aligned} S &= g_3(2R + S^2) + g_4(6RS + S^3) \\ R &= 1 + 2g_3RS + 3g_4R(R + S^2) \end{aligned} \tag{3.3}$$

4. Planar graphs and trees III: bipartite graphs

We now turn to the slightly more involved case of bipartite (i.e. vertex-bicolored, say black and white) graphs. In the language of matrix models, these correspond to the case of two coupled matrices.

4.1. p -valent case

Let us consider two-leg diagrams of vertex-bicolored p -valent planar graphs, and their generating functions with a weight g (resp. \tilde{g}) per p -valent black (resp. white) vertex. We must also indicate the color of the vertices to which the in and out-coming legs are attached, and this leads to a priori distinct generating functions. For simplicity, we restrict ourselves to only diagrams with incoming (resp. outgoing) leg attached to a white (resp. black) vertex with generating function $R \equiv R^{\circ}(g, \tilde{g})$, and also include the single graph whose incoming and outgoing legs are directly attached to one-another, without vertex, contributing 1 to R .

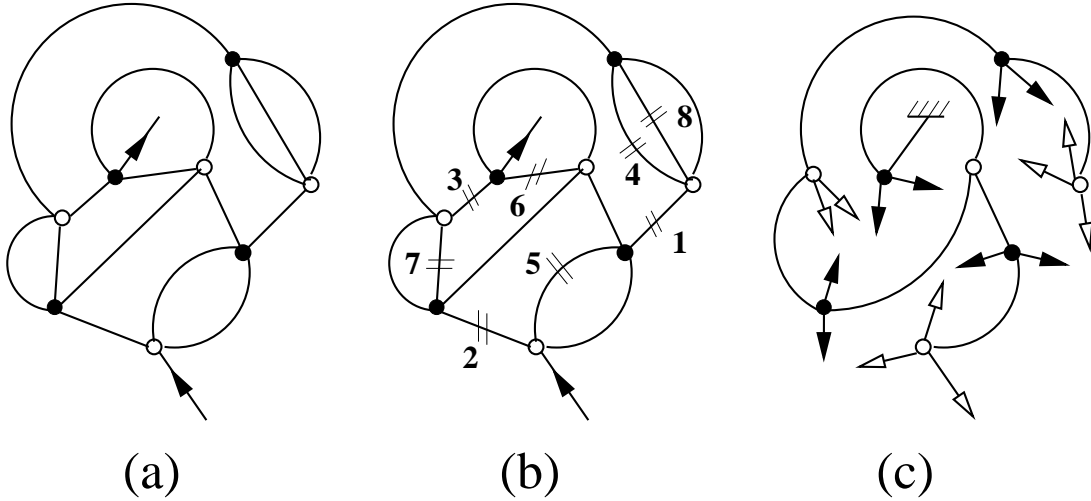


Fig.2: A sample bipartite p -valent two-leg diagram with $p = 4$ (a) is iteratively cut into a rooted bipartite blossom-tree (c) by the usual procedure, with the restriction that only edges originating from a black vertex may be cut. The edges to be cut are indicated in (b) with their order of visit, counterclockwise around the graph.

The above cutting procedure is now slightly modified, with the additional constraint that an edge may be cut only if it moreover originates from a black vertex (see Fig.2 for an illustration in the case $p = 4$). This leads to a new kind of blossom-trees (Fig.2 (c)), with bicolored vertices, and such that black or white leaves may only be connected to vertices of the same color, while each black vertex has exactly $p - 2$ black leaves attached to it. The tree still has the property of having one more white leaf than black ones (i.e. a total charge of $q = 1$), as the incoming leg is replaced by a white leaf (which is compatible with the above rule, as the incoming leg is attached to a p -valent white vertex). Moreover, the

root (former outcoming vertex) is attached to a black vertex. The generating function R obeys the relations:

$$\begin{aligned} R &= 1 + (p-1)gX \\ X &= \tilde{g}R^{p-1} \end{aligned} \tag{4.1}$$

The first line is obtained by inspection of all possible environments of the root: (i) it may simply have one white leaf attached to it or (ii) it may have a black vertex attached to it, itself with $p-2$ black leaves and a descendent rooted blossom-tree of total charge $+(p-1)$ with a black root, and with generating function X . The second line expresses these latter trees according to the environment of the white vertex attached to the root, having $p-1$ descendent rooted blossom-trees of charge $+1$, all generated by R . We finally get

$$R = 1 + (p-1)g\tilde{g}R^{p-1} \tag{4.2}$$

Note that the generating function $C_p(x)$ for rooted p -valent planar trees with a weight x per vertex satisfies $C_p(x) = 1 + xC_p(x)^{p-1}$ and $C_p(x) = 1 + O(x)$. The corresponding number of trees with N vertices reads $C_N^{(p)} = \frac{1}{1+(p-1)N} \binom{(p-1)N}{N}$. These numbers are also known as the Fuss-Catalan numbers, and reduce to the ordinary Catalan numbers for $p=3$. Finally the number of rooted blossom-trees with N vertices is simply $R|_{g^N \tilde{g}^N} = (p-1)^N C_N^{(p)}$. For large N , it behaves as $g_c^{-N}/N^{3/2}$, where $g_c = (p-2)^{p-2}/(p-1)^p$.

4.2. p -constellations

The p -constellations, introduced in [8], are vertex-bicolored (black and white) graphs such that say black vertices have all valence p , while white ones may have valences arbitrary multiples of p . We again consider two-leg diagrams of such planar graphs with say incoming leg connected to a white vertex and outcoming leg connected to a black vertex (see Fig.3 (a) for an illustration with $p=3$), or both legs being directly connected without vertex, and count them with a weight g per (p -valent) black vertex and weights \tilde{g}_m for mp -valent white vertices, $m=1,2,3\dots$. Let $R = R^{\circ\bullet}(g; \{\tilde{g}_i\})$ denote the corresponding generating function. The cutting procedure, illustrated in Fig.3, remains the same as in the previous section, and leaves us with rooted blossom-trees with bicolored vertices of total charge $+1$, such that leaves may only be connected to vertices of their own color, and that descendent subtrees may be of two types: if their first vertex is black, they have total charge 1; if its is white, they have total charge $p-1$, the descendents of the root vertex of the latter being

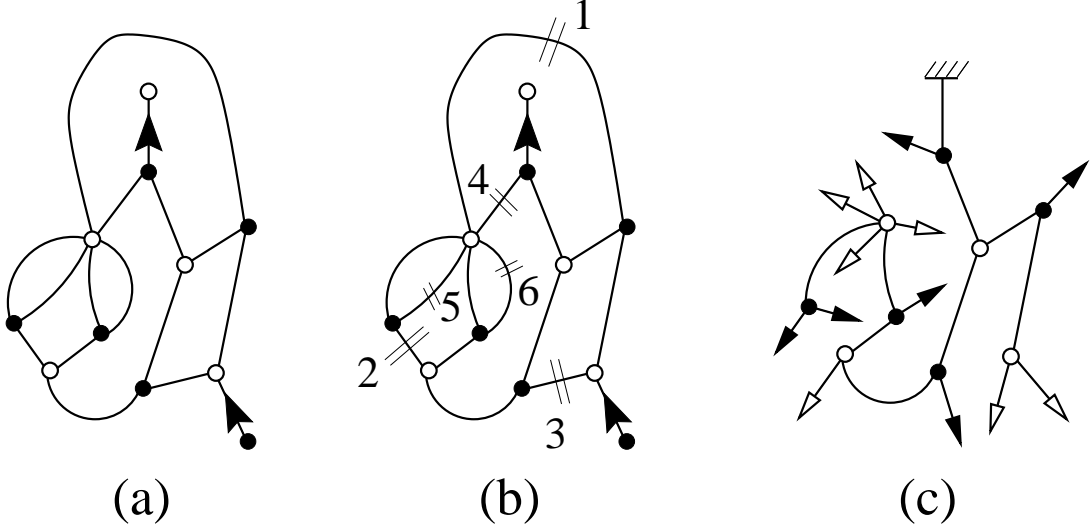


Fig.3: The cutting procedure is applied to a two-leg diagram of a 3-constellation (a), with incoming (resp. outgoing) leg attached to a white (resp. black) vertex. The edges are visited in counterclockwise order around the graph (b), and cut iff (i) this leaves the resulting graph connected (ii) the cut edge originates from a black vertex. We have indicated the chronological order of the cut edges, from 1 to 6. We finally replace each cut edge by a pair of black/white leaves, and the incoming (resp. outgoing) leg by a white leaf (resp. root).

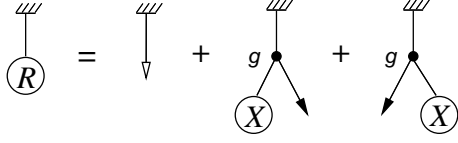
themselves only blossom trees of charge 1 or bunches of $p - 1$ black leaves attached to a black vertex.

By inspection of all possible local environments of the vertex attached to the root, we may derive the following relations for R :

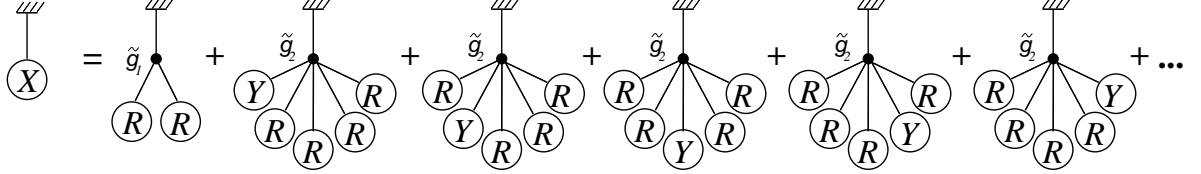
$$\begin{aligned}
 R &= 1 + (p - 1)gX \\
 X &= \sum_{m \geq 1} \tilde{g}_m \binom{mp - 1}{m - 1} Y^{m-1} R^{(p-1)m} \\
 Y &= g
 \end{aligned} \tag{4.3}$$

where R , X , Y generate rooted blossom-trees of respective charges 1, $p - 1$, $1 - p$, starting respectively with a black, white, black vertex. $Y = g$ is due to the fact that the only tree contributing to Y has a black vertex and $p - 1$ black leaves attached to it. In the case

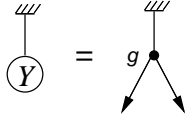
$p = 3$, this reads



$$R = 1 + 2gX$$



$$X = \tilde{g}_1 R^2 + 5\tilde{g}_2 Y R^4 + \dots$$



$$Y = g$$

(4.4)

Eliminating Y and X from (4.3), we arrive at the single algebraic equation

$$R = 1 + (p-1) \sum_{m \geq 1} \tilde{g}_m \binom{mp-1}{m-1} g^{m-1} R^{(p-1)m} \quad (4.5)$$

R is the unique solution to this equation such that $R = 1 + O(g, \tilde{g}_i)$.

Note that in the case $p = 2$ of 2-constellations, we recover the even-valent graph result (2.3), upon taking $g_{2k} = \tilde{g}_k$ for $k \geq 2$, while $\tilde{g}_1 = 0$ and $g = 1$. Indeed, in 2-constellations, the (2-valent) black vertices may be viewed as decorations of the edges of an arbitrary graph with only white even-valent vertices. Setting $g = 1$ precisely allows to forget about these decorations, while $\tilde{g}_1 = 0$ simply eliminates 2-valent white vertices.

4.3. Planar bipartite graphs and the Ising model

Constellations are easily tractable objects, essentially due to the triviality of one type of vertex (black here), whose valence remains fixed. More generally, we would like to consider in all generality vertex-bicolored graphs of arbitrary even valences for vertices of both colors. For the sake of simplicity, we will restrict ourselves to two-leg diagrams in which both legs are attached to white vertices. Let us denote by $R \equiv R^{\circ\circ}(\{g_{2i}\}; \{\tilde{g}_{2i}\})$ the generating function for two-leg diagrams of planar bipartite graphs with weights g_{2i} (resp. \tilde{g}_{2i}) per $2i$ -valent black (resp. white) vertex, $i = 1, 2, \dots$, and such that both legs are attached to white vertices.

Applying the now usual cutting procedure to two-leg diagrams, we end up with blossom-trees of total charge $+1$ with bicolored vertices of arbitrary even valences. Their characterization however is quite delicate, as it involves describing all their possible descendent subtrees. These come in two forms according to the color of their vertex attached to the root: if the latter is white, the possible descendent subtrees are either reduced to a black leaf (of charge -1) or rooted vertex-bicolored blossom trees of total charges $1, 3, 5, \dots$; if it is black, the possible descendent subtrees are rooted vertex-bicolored blossom trees of charges $1, -1, -3, -5, \dots$. Let us introduce the generating functions R_i for vertex-bicolored blossom-trees of total charge $2i - 1$, $i = 1, 2, 3, \dots$ and whose root is attached to a white vertex, together with the generating functions X_i for vertex-bicolored blossom-trees of total charge $1 - 2i$, $i = 1, 2, 3, \dots$ and whose root is attached to a black vertex, while $V \equiv X_0$ generates vertex-bicolored blossom-trees of total charge 1 and whose root is attached to a black vertex, or the tree made of a single leaf attached to the root, without any vertex (contributing 1 to V). We also introduce the generating function $R_0 = 1$ for the tree made of a single black leaf attached to the root, without any vertex. We now simply have to enumerate all possible environments of the vertex attached to the root of each of these trees, according to the type of its attached descendent subtrees. This gives the following system

$$\begin{aligned}
V &= 1 + \sum_{k \geq 1} g_{2k} \sum_{\substack{j_1, j_2, \dots, j_{2k-1} \geq 0 \\ \Sigma j_l = k}} R_{j_1} R_{j_2} \dots R_{j_{2k-1}} \\
X_m &= \sum_{k \geq 1} g_{2k} \sum_{\substack{j_1, j_2, \dots, j_{2k-1} \geq 0 \\ \Sigma j_l = k-m}} R_{j_1} R_{j_2} \dots R_{j_{2k-1}}, \quad m = 1, 2, 3, \dots \\
R_m &= \sum_{k \geq 1} \tilde{g}_{2k} \sum_{\substack{j_1, j_2, \dots, j_{2k-1} \geq 0 \\ \Sigma j_l = k-m}} X_{j_1} X_{j_2} \dots X_{j_{2k-1}}, \quad m = 1, 2, 3, \dots
\end{aligned} \tag{4.6}$$

The desired generating function $R = R_1$ is the unique solution to this system where all R 's, X 's and V admit power series expansions of the g 's and \tilde{g} 's.

The case of the Ising model on planar tetravalent graphs may be viewed as a particular case of the above, in which only $g_2, g_4, \tilde{g}_2, \tilde{g}_4$ are non-zero. To see this, recall that the Ising model on tetravalent planar graphs is defined by say coloring the vertices of an arbitrary tetravalent planar graph in black or white (colors stand here for the spin up or down), and counting the configurations with different ‘‘nearest neighbor interaction’’ weights for edges connected to vertices of the same color (weight e^K) or of different colors (weight 1), while

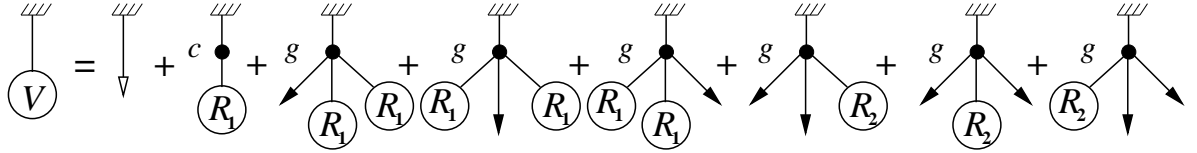
black (resp. white) vertices are counted with a weight ge^H (resp. ge^{-H}). Here K and H are respectively the spin coupling and the external magnetic field of the Ising model. To make the contact with our model, we just have to resum all possible configurations obtained by adding arbitrary numbers of 2-valent black and white vertices on the edges of Ising configurations, in such a way that bicoloration is restored. This entails adding any chain of black, white, black, ..., white 2-valent vertices between any white and black tetravalent vertices connected by an edge, or any chain of alternating white, black, ..., white 2-valent vertices between any two black tetravalent vertices connected by an edge or else any chain of black, white, ..., black 2-valent vertices between any two white tetravalent vertices connected by an edge. Doing the resummations within the configurations of our bicolored graphs produces an effective edge interaction weight w_{ab} according to the colors a, b of the adjacent vertices:

$$\begin{aligned}
w_{\bullet\bullet} &= \frac{\tilde{g}_2}{1 - g_2\tilde{g}_2} = \bullet\text{---}\circ\text{---}\bullet + \bullet\text{---}\circ\text{---}\bullet\text{---}\circ\text{---}\bullet + \dots \\
w_{\circ\circ} &= \frac{g_2}{1 - g_2\tilde{g}_2} = \circ\text{---}\bullet\text{---}\circ + \circ\text{---}\bullet\text{---}\circ\text{---}\bullet\text{---}\circ + \dots \\
w_{\bullet\circ} &= w_{\circ\bullet} = \frac{1}{1 - g_2\tilde{g}_2} = \circ\text{---}\bullet + \circ\text{---}\bullet\text{---}\circ\text{---}\bullet + \dots
\end{aligned} \tag{4.7}$$

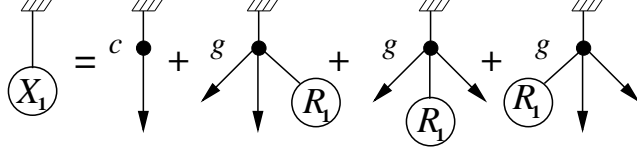
hence to identify our model with the Ising one, we must take $g_2 = \tilde{g}_2 = e^K$, while $g_4 = (1 - e^{2K})^2 ge^H$ and $\tilde{g}_4 = (1 - e^{2K})^2 ge^{-H}$, and the external legs must receive the extra weights $1/\sqrt{1 - e^{2K}}$ each.

Restricting to the symmetric case $g_2 = \tilde{g}_2 \equiv c$ and $g_4 = \tilde{g}_4 \equiv g$, the above equations

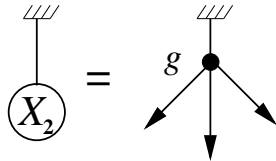
simply read



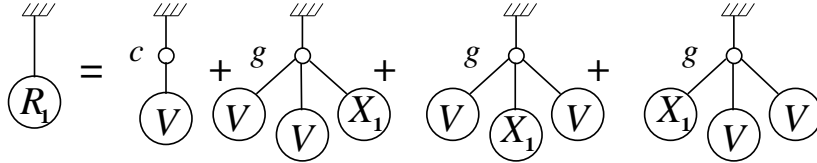
$$V = 1 + cR_1 + 3gR_1^2 + 3gR_2$$



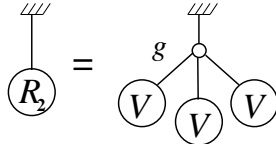
$$X_1 = c + 3gR_1$$



$$X_2 = g$$



$$R_1 = cV + 3gV^2X_1$$



$$R_2 = gV^3$$

(4.8)

Eliminating R_2 and X_1 , we get

$$V = \frac{R}{c + 3gR} \quad \text{with} \quad R(c + 3gR)^2(1 - (c + 3gR)^2) = (c + 3gR)^3 + 3g^2R^3 \quad (4.9)$$

Here, $R \equiv R_1$ is the generating function for two-leg diagrams of planar tetravalent graphs with Ising (black or white) spins decorating their vertices, with interaction weights $w_{\bullet\bullet} = w_{\circ\circ} = c$, $w_{\bullet\circ} = w_{\circ\bullet} = 1$ and a weight $g/(1 - c^2)^2$ per tetravalent vertex, and such that the two legs are attached to univalent black vertices, themselves weighted by $1/\sqrt{1 - c^2}$.

5. Geodesic distances

In the previous sections, we have enumerated various one- and two-leg diagrams by establishing bijections with suitable classes of blossom-trees. Note that in the plane rep-

resentation we have chosen, the face F_1 adjacent to the unique leg for one-leg diagrams is not necessarily the external face F_0 . Accordingly in the case of two-leg diagrams, the face F_1 adjacent to the out-coming leg need not be the external face F_0 , itself adjacent to the in-coming leg. In this section, we show how to keep track of the *geodesic distance* between F_0 and F_1 , namely the smallest number of edges to be crossed in a path from F_0 to F_1 . By a slight abuse of language, this distance will also be referred to as the distance between the legs.

5.1. Keeping track of the geodesic distances

The main feature of the previous sections is a sort of unified formulation of planar graphs in the language of blossom-trees. Note that going back from blossom-trees to graphs is a straightforward step, as there is a unique way of reconnecting the black and white leaves into edges: this is done by simply connecting each black leaf to the first available white leaf in counterclockwise direction. This process leaves us in the case of trees of charge 1 with exactly one unmatched white leaf, which is taken as outcoming leg, while the root is the incoming one. For trees of charge 0, all pairs are exhausted and only the root remains as unique leg. In both cases, we note that the geodesic distance between the faces F_0 (external) and F_1 (adjacent to the former root) is simply given by the number of black-white edge pairs that separate the root from the external face after recombination. Keeping track of this geodesic distance simply amounts to keeping track of the black leaves “in excess” that require encompassing the root to be connected to their white *alter ego*.

This is done in all generality by attaching to each blossom-tree a “contour walk”, namely a walk on the relative integer line with steps ± 1 , obtained as follows (see Fig.4 for an example). One starts from the root of the blossom-tree and visits in clockwise direction all leaves around the tree. Starting from the coordinate 0, we make a step $+1$ (resp. -1) for each encountered black (resp. white) leaf. In a blossom-tree of charge k , such a walk will end up at coordinate $-k$. Now the number of excess black leaves responsible for the geodesic distance between F_1 and F_0 is simply the maximum coordinate reached by the contour walk.

In view of this result, and of the form of all relations determining the blossom-trees of the previous sections, it is natural to introduce by analogy with the generating functions say X for some particular type of blossom-trees the generating function X_n for the same blossom-trees with a geodesic distance of at most n between F_1 and F_0 . To obtain from X_n the generating function for blossom-trees with geodesic distance equal to n between F_0

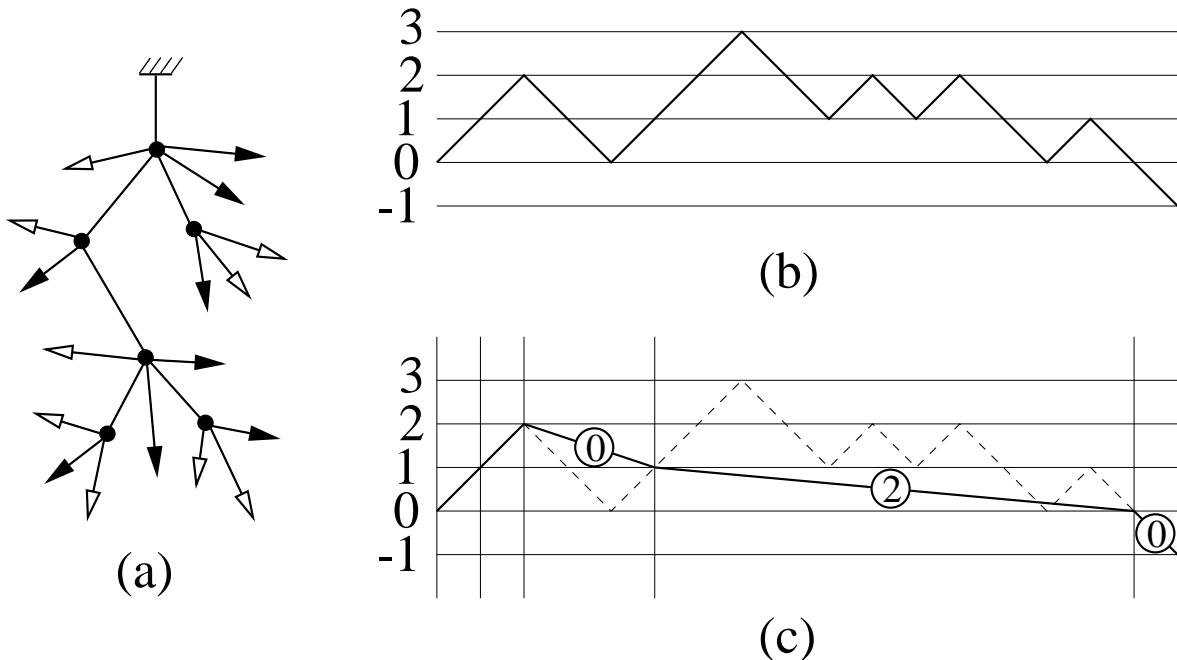


Fig.4: The contour walk of a rooted blossom-tree. Visiting the tree (a) in clockwise direction starting from the root, one keeps a record of the type of leaves encountered in the form of a walk on the integer line (b), starting at the origin, and with steps up (for a black leaf) and down (for a white one). The maximum reached by the walk is nothing but the geodesic distance separating the root from the external face in the recombined graph. This distance is 3 in the present case, as one readily checks by closing the tree back into a planar graph (with tetra/hexavalent vertices here). Concentrating on the environment of the vertex attached to the root, we see that each descendent subtree corresponds to a portion of the walk (c), with a certain relative maximum. Expressing the global maximum of the contour walk in terms of the relative maxima of its portions allows for writing a recursion relation for the generating function for rooted blossom-trees whose root is at a maximum distance n from the external face of the recombined graph.

and F_1 , we simply have to take the difference $X_n - X_{n-1}$. Keeping track of n then boils down to expressing the maximum of the contour walk of a tree in terms of those of the individual contour walks of the blossom-trees descending from the vertex attached to the root, following the same inspection procedure as before. This is done case by case in the following sections.

5.2. Even valences

Let us start with the tetravalent case. We find that eq. (2.1) must be transformed into

$$R_n = 1 + gR_n(R_{n-1} + R_n + R_{n+1}) \quad (5.1)$$

where R_n denotes the generating function for tetravalent planar graphs with two legs at distance at most n , and weight g per vertex. The three terms on the r.h.s. correspond to respectively the black leaf on the right, in the middle or on the left of the two other descendents of the vertex attached to the root (see the picture of eq.(2.1)). It is clear that the presence of the black leaf acts as a shift by -1 on the local distance n while R_n accompanies a shift by $+1$, when going clockwise around the vertex.

To have a compact notation for the general result, let us introduce a formal orthonormal basis $|n\rangle$, $n \in \mathbb{Z}$, with $\langle m|n\rangle = \delta_{m,n}$, and an operator σ acting as a shift $\sigma|n\rangle = |n+1\rangle$, and its formal inverse σ^{-1} such that $\sigma^{-1}|n\rangle = |n-1\rangle$. We introduce the operator

$$Q = \sigma + \sigma^{-1}\hat{r} \quad (5.2)$$

where \hat{r} simply acts diagonally as $\hat{r}|n\rangle = R_n|n\rangle$. Note that the shift σ may be represented by a black leaf, while its inverse always accompanies an R . Then eq. (5.1) takes the form

$$1 = \langle n-1|(Q - gQ^3)|n\rangle \quad (5.3)$$

More generally, in the case of arbitrary even valences, we have to write

$$1 = \langle n-1|(Q - \sum_{k \geq 2} g_{2k} Q^{2k-1})|n\rangle \quad (5.4)$$

For instance in the case of tetra- and hexa-valent graphs, eq. (5.3) reads explicitly

$$\begin{aligned} R_n = & 1 + g_4 R_n (R_{n+1} + R_n + R_{n-1}) + g_6 R_n (R_{n+1} R_{n+2} + R_{n+1} R_{n-1} \\ & + R_{n-1} R_{n-2} + R_{n+1}^2 + R_{n-1}^2 + R_n (2R_{n+1} + R_n + 2R_{n-1})) \end{aligned} \quad (5.5)$$

A remark is in order. The equations (5.1)-(5.5) are valid only for $n \geq 0$, provided we use $R_{-k} = 0$, $k = 1, 2, \dots$ wherever they occur in the r.h.s. With these boundary conditions, and the general fact that R_n possess a power series expansion in g , with $R_n = 1 + O(g)$ for $n \geq 0$, all R_n 's are then uniquely determined by (5.4) order by order in g .

5.3. Arbitrary valences

Let S_n (resp. R_n) denote the generating function for one- (resp. two-) leg diagrams of planar graphs with arbitrary valences with weights g_i per i -valent vertex, and such that F_0 (the external face) and F_1 (the face adjacent to the unique (resp. outgoing) leg) are

distant by at most n . For trivalent graphs, we find that eqs. (3.1) must be transformed into

$$\begin{aligned} S_n &= g(R_n + R_{n-1}) + gS_n^2 \\ R_n &= 1 + gR_n(S_{n+1} + S_n) \end{aligned} \quad (5.6)$$

where in addition to the situation of previous section we simply note that S 's don't affect the distance counting (no shift). This suggests to introduce in the general case of arbitrary valences the operator

$$Q = \sigma + \sigma^{-1}\hat{s}\sigma + \sigma^{-1}\hat{r} \quad (5.7)$$

where \hat{s} acts diagonally on the basis $|n\rangle$ as $\hat{s}|n\rangle = S_n|n\rangle$, and in terms of which we simply have to write

$$\begin{aligned} 0 &= \langle n|(Q - \sum_{i \geq 3} g_i Q^{i-1})|n\rangle \\ 1 &= \langle n-1|(Q - \sum_{i \geq 3} g_i Q^{i-1})|n\rangle \end{aligned} \quad (5.8)$$

For tri- and tetra-valent graphs, this reads

$$\begin{aligned} S_n &= g_3(R_n + R_{n-1} + S_n^2) + g_4(R_n(S_{n+1} + 2S_n) + R_{n-1}(S_{n-1} + 2S_n) + S_n^3) \\ R_n &= 1 + g_3R_n(S_n + S_{n+1}) + g_4R_n(S_n^2 + S_nS_{n+1} + S_{n+1}^2 + R_{n+1} + R_n + R_{n-1}) \end{aligned} \quad (5.9)$$

Note that when $g_3 = 0$, we find the solution $S_n = 0$ identically, and eq. (5.9) reduces to the tetravalent case (5.1). More generally, imposing that all odd g 's vanish leads to the solution $S_n = 0$ (as there are no one-leg diagrams with only even valences), and we recover the even-valent case of previous section.

5.4. Constellations

Let R_n denote the generating function for two-leg diagrams of p -constellations with a weight g per white (p -valent) vertex, and weights \tilde{g}_i per black pi -valent vertex, $i = 1, 2, \dots$, whose incoming (resp. outgoing) leg is attached to a black (resp. white) vertex (or both are connected without vertex and the corresponding unique graph contributes 1 to R_n for all n) and such that the geodesic distance between the two legs is at most n . Here the notion of geodesic distance is defined according to the rules used in the cutting procedure of Sect.5.3, namely the geodesic distance between F_0 and F_1 is the minimal number of edges to be crossed in a path going from F_0 to F_1 , and such that at each edge-crossing the white vertex is always on the right. Following the same reasoning as in the previous sections, we are now led to the introduction of two operators Q_1 and Q_2 which generate, upon taking

powers, the successive decorations of the vertex attached to the root, respectively in the case of a black and white vertex. We have

$$\begin{aligned} Q_1 &= \sigma + \sigma^{-1} \hat{x} \sigma^{2-p} \\ Q_2 &= \sigma^{-1} \hat{r} + \sigma^{p-2} \hat{y} \sigma \end{aligned} \tag{5.10}$$

where the shift σ represents a single black leaf, while \hat{x} represents rooted blossom-trees of charge $p-1$ whose first vertex is white. Again, $\hat{x}, \hat{y}, \hat{r}$ act diagonally on the basis $|n\rangle$ with eigenvalues X_n, Y_n, R_n respectively. The equations (4.3) now become

$$\begin{aligned} 1 &= \langle n-1 | (Q_2 - gQ_1^{p-1}) | n \rangle \\ 0 &= \langle n+p-1 | (Q_2 - gQ_1^{p-1}) | n \rangle \\ 0 &= \langle n-p+1 | (Q_1 - \sum_{i \geq 1} \tilde{g}_i Q_2^{pi-1}) | n \rangle \end{aligned} \tag{5.11}$$

In the particular case of 3-constellations, with say only $g, \tilde{g}_1, \tilde{g}_2$ non-zero, these read for instance

$$\begin{aligned} R_n &= 1 + g(X_n + X_{n-1}) \\ Y_n &= g \\ X_n &= \tilde{g}_1 R_n R_{n+1} + \tilde{g}_2 g R_n R_{n+1} (R_{n+3} R_{n+2} + R_{n+2} R_{n+1} + R_{n+1} R_n + R_n R_{n-1}) \end{aligned} \tag{5.12}$$

while in the case of only (black and white) p -valent vertices of Sect. 4.1, eqs.(5.11) read

$$\begin{aligned} R_n &= 1 + g(X_n + X_{n-1} + \dots + X_{n-p+2}) \\ X_n &= \tilde{g}_1 R_n R_{n+1} \dots R_{n+p-2} \end{aligned} \tag{5.13}$$

for the generating function R_n for two-leg-diagrams of bipartite p -valent graphs with incoming leg attached to a white vertex and outgoing leg attached to a black one, and such that the geodesic distance from the in- to the out-coming leg is at most n .

5.5. Bipartite even-valent graphs and the Ising model

In the general case of bipartite even-valent graphs, we are led to the introduction of two operators Q_1, Q_2 with the following structure

$$\begin{aligned} Q_1 &= \sigma + \sum_{k \geq 1} \sigma^{1-2k} \hat{r}^{(k)} \\ Q_2 &= \sigma^{-1} \hat{v} + \sum_{k \geq 1} \sigma^{-1} \hat{x}^{(k)} \sigma^{2k} \end{aligned} \tag{5.14}$$

where the $\hat{r}^{(k)}, \hat{x}^{(k)}, \hat{v}$ all act diagonally with eigenvalues $R_n^{(k)}, X_n^{(k)}, V_n$. The latter are nothing but the generating functions for sets of rooted blossom-trees restricted by n , respectively starting with a white, black, black vertex, and with charges $2k - 1, 1 - 2k, 1$ respectively. We are actually interested in computing $R_n \equiv R_n^{(1)}$, the generating function for two-leg diagrams of bipartite planar graphs with weights g_{2i}, \tilde{g}_{2i} per $2i$ -valent black, white vertex, such that moreover the two legs are distant by at most n . Again, the distance from F_0 to F_1 is defined as the minimal number of edges to be crossed in a path from F_0 to F_1 , such that at each edge crossing the white vertex is always on the right. This definition allows to keep track of this distance on the trees themselves, as the number of “excess” black leaves which upon recombination with white ones encompass the root of the tree. The equations determining R_n are simply

$$\begin{aligned} 1 &= \langle n-1 | (Q_2 - \sum_{i \geq 1} g_{2i} Q_1^{2i-1}) | n \rangle \\ 0 &= \langle n+2m-1 | (Q_2 - \sum_{i \geq 1} g_{2i} Q_1^{2i-1}) | n \rangle, \quad m = 1, 2, \dots \\ 0 &= \langle n-2m+1 | (Q_1 - \sum_{i \geq 1} \tilde{g}_{2i} Q_2^{2i-1}) | n \rangle, \quad m = 1, 2, \dots \end{aligned} \quad (5.15)$$

In the abovementioned case of the Ising model with only $g_2 = \tilde{g}_2 = c$ and $g_4 = \tilde{g}_4 = g$ non-zero, we must take $Q_1 = \sigma + \sigma^{-1} \hat{r}^{(1)} + \sigma^{-3} \hat{r}^{(2)}$ and $Q_2 = \sigma^{-1} \hat{v} + \sigma^{-1} \hat{x}^{(1)} \sigma^2 + \sigma^{-1} \hat{x}^{(2)} \sigma^4$, and eq.(5.15) reduces to

$$\begin{aligned} V_n &= 1 + cR_n + gR_n(R_{n+1} + R_n + R_{n-1}) + g(R_n^{(2)} + R_{n+1}^{(2)} + R_{n+2}^{(2)}) \\ X_n^{(1)} &= c + g(R_n + R_{n-1} + R_{n-2}) \\ X_n^{(2)} &= g \\ R_n &= cV_n + gV_n(V_{n+1}X_{n+2}^{(1)} + V_nX_{n+1}^{(1)} + V_{n-1}X_n^{(1)}) \\ R_n^{(2)} &= gV_nV_{n-1}V_{n-2} \end{aligned} \quad (5.16)$$

We first remark that $R_n = V_n X_{n+1}^{(1)}$ by comparing the second and fourth lines of eq.(5.16). This is a particular case of a general duality between Q_1 and Q_2 in the symmetric case when $g_i = \tilde{g}_i$ for all i , where we may write $Q_1 = Q_2^\dagger$, where $\sigma^\dagger = \sigma^{-1}v$, $(AB)^\dagger = B^\dagger A^\dagger$ for all operators A, B , and $f^\dagger = f$ for all diagonal operators. Here this implies $\sigma^{-1}x^{(1)}\sigma^2 = r^{(1)}v^{-1}\sigma$ and $\sigma^{-1}x^{(2)}\sigma^4 = r^{(2)}(v^{-1}\sigma)^3$, i.e. $R_n = V_n X_{n+1}^{(1)}$ and $R_n^{(2)} = X_{n+1}^{(2)} V_n V_{n-1} V_{n-2}$. Finally eliminating $X_n^{(1)}$ and $R_n^{(2)}$ from eq.(5.16), we are left with

$$\begin{aligned} V_n(1 - g^2(V_{n+1}V_{n+2} + V_{n+1}V_{n-1} + V_{n-1}V_{n-2})) &= 1 + R_n(c + g(R_{n+1} + R_n + R_{n-1})) \\ R_n &= V_n(c + g(R_{n+1} + R_n + R_{n-1})) \end{aligned} \quad (5.17)$$

An important remark is in order about the generating function R_n . Although n has the meaning of a maximal geodesic distance between the two legs in the bipartite graph picture, it loses somewhat of its meaning in the correspondence with Ising model configurations. Indeed, within configurations of the Ising model on tetravalent planar graphs, n is not the obvious geodesic distance between the faces adjacent to the in- and out-coming legs, as its definition involves first transforming the graph into a bipartite one, and it then corresponds to a distance where edge-crossing is permitted only if the white vertex is on the right. This restriction is almost irrelevant, as there are in general sufficiently many successions of black, white, black... bivalent vertices to allow for crossing edges in both directions. One case however is troublesome: when an Ising edge connects a black vertex to a white one, in the absence of intermediate bivalent vertices (not necessary here as the bicolouration is already ensured), the edge may only be crossed in one direction, leaving the white vertex on the right. This introduces a bias in the notion of distance, having to do with the matter configurations on the graph. An analogous situation was encountered in [11] [15] in the case of hard dimers on tetravalent planar graphs, namely on configurations of tetravalent planar graphs where edges may (or may not) be occupied by dimers which repel one-another in such a way that no two adjacent edges can be simultaneously occupied. In this case indeed, the notion of geodesic distance is biased by the dimers, in that the occupied edges cannot be crossed in paths from F_0 to F_1 . In both Ising and hard-dimer cases, the matter interferes with the space, by modifying the rules governing distances. Consequently, we think it is interesting to investigate the dependence of the Ising two-leg diagrams on this special distance, and it may eventually be that its difference with the true geodesic distance becomes irrelevant in large graphs.

6. Exact solutions

6.1. Finding exact solutions: a general scheme

All the equations listed in Sect. 5, despite their diversity, are all basically of the same form: (possibly coupled) algebraic recursion relations expressing R_n (and the other generating functions involved) in terms of a finite number of previous terms $R_{n-1}, R_{n-2}, \dots, R_{n-k}$. In principle the boundary data needed to entirely determine R_n should consist of k consecutive initial values of R_j . It turns out however that we may drastically simplify, namely divide by 2 this required number of initial data by simply requiring that $\lim_{n \rightarrow \infty} R_n$ exists, and that it moreover coincides with the generating function R . Indeed, this is nothing but

restating the definitions of R_n and R , as the latter was first obtained regardless of the geodesic distance between legs, while the limit $n \rightarrow \infty$ of the former amounts to removing the geodesic distance constraint in the counting of graphs. In the same fashion, all other generating functions involved tend to their obvious limiting values when $n \rightarrow \infty$. This allows to linearize the various recursion relations at large n , by setting say $R_n = R - \rho_n$, and similarly for the other generating functions involved. At first order in ρ_n and its other counterparts, we obtain (possibly coupled) linear recursion relations. We immediately deduce that $\rho_n \sim x^n$ (or a linear combination involving x 's of the same modulus) for some solution x (with modulus less than 1) to the characteristic equation of the linearized recursion relations.

To completely solve our equations, we start by determining the exact form of the linearized solution, in general a linear combination $\rho_n \sim \sum_{j=1}^k a_j (x_j)^n$ where $x_j, j = 1, 2, \dots, k$ denote all the (generically distinct) solutions of the linearized characteristic equation with modulus less than 1. In a second step, we obtain order by order in the $(x_j)^n$ the higher order contributions to the true solution, expanded at large n . These take in general the form of recursion relations for the coefficients of the multiple expansion in powers of the $(x_j)^n$. Solving these recursion relations, and resumming the resulting series allows us to finally obtain compact expressions for the exact solutions to the non-linear recursion relations at hand. The result still depends on the initial parameters $a_j, j = 1, 2, \dots, k$, which then are fixed by requiring that the terms involving the k first $R_{-k}, R_{-k+1}, \dots, R_{-1}$ drop out of the recursion relations.

In the following sections, we simply present the solutions, as we have found them. A case by case proof by substitution is left as an exercise to the reader. In many situations, the proof boils down to a certain identity between Chebyshev polynomials of the first kind, as will be apparent soon.

6.2. Tetravalent case

For pedagogical purposes, we detail in this simple case the general scheme presented in the previous section. Substituting $R_n = R - \rho_n$ into eq.(5.1) we get at first order in ρ_n :

$$\rho_n(1 - 3gR) = gR(\rho_{n-1} + \rho_n + \rho_{n+1}) + O(\rho_n^2) \quad (6.1)$$

The linearized characteristic equation therefore reads

$$1 - gR \left(x + \frac{1}{x} + 4 \right) = 0 \quad (6.2)$$

For $g < g_c = 1/12$, there is generically a unique solution $x \equiv x(g)$ with modulus less than 1 to this equation, and we find that at first order $\rho_n = ax^n + O(x^{2n})$. We may now infer the general form $\rho_n = \sum_{j \geq 1} a_j x^{nj}$, $a_1 = a$ for the complete solution, where the coefficients a_j are to be determined order by order in x^n . We find explicitly

$$a_{k+1} = \sum_{j=1}^k \left(\frac{x^j + \frac{1}{x^j} + 1}{x^{k+1} + \frac{1}{x^{k+1}} - x - \frac{1}{x}} \right) a_j a_{k+1-j} \quad (6.3)$$

solved recursively as

$$a_k = a \frac{1 - x^k}{1 - x} \left(\frac{ax}{(1-x)(1-x^2)} \right)^{k-1} \quad (6.4)$$

Picking $a = x(1-x)(1-x^2)\lambda$, R_n is easily resummed into

$$R_n = R \frac{u_n u_{n+3}}{u_{n+1} u_{n+2}}, \quad u_n = 1 - \lambda x^{n+1} \quad (6.5)$$

This is the general solution to eq.(5.1), that converges for large n . To see why, it is simplest to substitute the form (6.5) into the initial equation (5.1) which then boils down to the following quartic relation

$$u_n u_{n+1} u_{n+2} u_{n+3} = \frac{1}{R} u_{n+1}^2 u_{n+2}^2 + gR (u_{n-1} u_{n+2}^2 u_{n+3} + u_n^2 u_{n+3}^2 + u_n u_{n+1}^2 u_{n+4}) \quad (6.6)$$

Substituting $u_n = 1 - \lambda x^{n+1}$ into this, we just have to check that the zeros of the l.h.s. as a degree 4 polynomial in $\Lambda = \lambda x^n$ match those of the r.h.s. as moreover the equation reduces to eq. (2.1) for $\Lambda = 0$.

Finally, the ‘‘integration’’ constant λ is now fixed by further requiring that eq.(5.1) makes sense at $n = 0$, in which case the term R_{-1} must drop off the r.h.s. of the recursion relation, in other words we have to impose $R_{-1} = 0$. This simply gives $\lambda = 1$, and finally the exact solution to our combinatorial problem reads

$$R_n = R \frac{(1 - x^{n+1})(1 - x^{n+4})}{(1 - x^{n+2})(1 - x^{n+3})} = R \frac{U_n U_{n+3}}{U_{n+1} U_{n+2}}, \quad U_n \equiv U_n \left(\sqrt{x} + \frac{1}{\sqrt{x}} \right) = \frac{x^{\frac{n+1}{2}} - x^{-\frac{n+1}{2}}}{x^{\frac{1}{2}} - x^{-\frac{1}{2}}} \quad (6.7)$$

where we have identified the Chebyshev polynomials U_n of the first kind.

As a simple application, the formula (6.7) gives access to the generating function for two-leg diagrams whose legs lie in the same face, already identified as that of rooted tetravalent planar maps or quadrangulations. We find that

$$R_0 = R \frac{x + \frac{1}{x}}{x + \frac{1}{x} + 1} = R \frac{1 - 4gR}{1 - 3gR} = R - gR^3 \quad (6.8)$$

with R as in (2.2). This result was first obtained by Tutte [4] in a completely different, though combinatorial, manner.

6.3. Even valences

Let us for definiteness consider the equation (5.4) with only $g_4, g_6, \dots, g_{2m+2}$ non-zero. Linearizing again the equation at large n and solving for the leading $\rho_n \sim x^n$, we find that x must obey the following characteristic equation:

$$\begin{aligned} 0 = \chi_m(x) &\equiv 1 - \sum_{k=0}^m g_{2k+2} R^k \sum_{l=0}^k \binom{2k+1}{l} \frac{1}{x^{k-l}} \frac{1 - x^{2k+1-2l}}{1-x} \\ &= 1 - \sum_{k=1}^m g_{2k+2} R^k \sum_{l=0}^k \binom{2k+1}{l} U_{2k-2l}(w) \end{aligned} \quad (6.9)$$

expressed in terms of Chebyshev polynomials of $w = \sqrt{x} + 1/\sqrt{x}$. Note that $\chi_m(x)$ is actually a degree m polynomial in $x + 1/x$, with generically m distinct roots with modulus less than 1, denoted by x_1, x_2, \dots, x_m . Repeating the straightforward, though tedious, exercise of previous section, we end up with the following exact solution

$$\begin{aligned} R_n &= R \frac{u_n^{(m)} u_{n+3}^{(m)}}{u_{n+1}^{(m)} u_{n+2}^{(m)}} \\ u_n^{(m)} &= \sum_{l=0}^m (-1)^l \sum_{1 \leq m_1 < \dots < m_l \leq m} \prod_{i=1}^l \lambda_{m_i} x_{m_i}^{n+m} \prod_{1 \leq i < j \leq l} c_{m_i, m_j} \\ c_{a,b} &\equiv \frac{(x_a - x_b)^2}{(1 - x_a x_b)^2} \end{aligned} \quad (6.10)$$

Remarkably, the structure of $u_n^{(m)}$ matches exactly that of an N -soliton tau-function of the KP hierarchy [19] which reads

$$\begin{aligned} \tau &= \sum_{r=0}^N \sum_{i_1 < \dots < i_r} \prod_{\mu=1}^r e^{\eta_{i_\mu}} \left(\prod_{\mu < \nu} c_{i_\mu, i_\nu} \right) \\ c_{i,j} &= \frac{(p_i - p_j)(q_i - q_j)}{(p_i - q_j)(q_i - p_j)} \end{aligned} \quad (6.11)$$

where the η 's contain the times' dependence of the KP hierarchy. Our solution (6.10) simply amounts to identifying $N = m$, $e^{\eta_i} = -x_i^{n+m} \lambda_i$, $p_i = x_i$ and $q_i = 1/x_i$, $i = 1, 2, \dots, m$. This surprising relation suggests the existence of an underlying integrable structure for our recursion relations, but remains mysterious.

Again, to further fix the ‘‘integration constants’’ $\lambda_1, \lambda_2, \dots, \lambda_m$, we simply have to express that $u_{-1} = u_{-2} = \dots = u_{-m} = 0$, with the result

$$\lambda_i = \prod_{j \neq i} \frac{1 - x_i x_j}{x_i - x_j} \quad i = 1, 2, \dots, m \quad (6.12)$$

and finally the complete solution to (5.4) reads

$$R_n = R \frac{U_n(w_1, \dots, w_m) U_{n+3}(w_1, \dots, w_m)}{U_{n+1}(w_1, \dots, w_m) U_{n+2}(w_1, \dots, w_m)} \quad (6.13)$$

where

$$U_n(w_1, \dots, w_m) \equiv \det [U_{n+2j-2}(w_i)]_{1 \leq i, j \leq m} \quad (6.14)$$

in terms of Chebyshev polynomials of the first kind expressed at the values $w_i = \sqrt{x_i} + 1/\sqrt{x_i}$, $i = 1, 2, \dots, m$. The precise proof of these statements can be found in [15].

For illustration, in the tetra/hexavalent case $m = 2$, we have the characteristic equation

$$0 = \chi_2(x) \equiv 1 - g_4 R \left(x + \frac{1}{x} + 4 \right) - g_6 R^2 \left(x^2 + 6x + 16 + \frac{6}{x} + \frac{1}{x^2} \right) \quad (6.15)$$

and for instance the result (6.13)(6.14) reads for $n = 0$:

$$R_0 = R \frac{1 + (x_1 + \frac{1}{x_1})(x_2 + \frac{1}{x_2})}{1 + (1 + x_1 + \frac{1}{x_1})(1 + x_2 + \frac{1}{x_2})} = R \frac{1 - 4g_4 R - 15g_6 R^2}{1 - 3g_4 R - 10g_6 R^2} \quad (6.16)$$

where we have reexpressed the symmetric functions of $x_1 + 1/x_1$ and $x_2 + 1/x_2$ in terms of the coefficients of $\chi_2(x)$. The result is nothing but the generating function for rooted tetra/hexavalent planar graphs.

6.4. Trivalent case

Repeating the exercise of Sect.6.2 for the trivalent case of eqs. (5.6), we have found the following solution

$$R_n = R \frac{u_n u_{n+2}}{u_{n+1}^2}, \quad u_n = 1 - \lambda x^{n+1} \quad (6.17)$$

while

$$S_n = S - \frac{t_n}{u_n u_{n+1}}, \quad t_n = g R^2 (1 - x)(1 - x^2) \lambda x^n \quad (6.18)$$

In eqs.(6.17)(6.18), the parameter x is the unique solution to the linearized characteristic equation

$$1 - g^2 R^3 \left(x + \frac{1}{x} + 2 \right) = 0 \quad (6.19)$$

such that $|x| < 1$.

Requiring that $R_{-1} = 0$, fixes $\lambda = 1$, and we obtain the complete solution

$$\begin{aligned} R_n &= R \frac{(1 - x^{n+1})(1 - x^{n+3})}{(1 - x^{n+2})^2} \\ S_n &= S - gR^2 \frac{(1 - x)(1 - x^2)x^n}{(1 - x^{n+1})(1 - x^{n+2})} \end{aligned} \quad (6.20)$$

from which we read off the following compact expressions for R_0 and S_0 , respectively generating two- and one-leg diagrams of trivalent planar graphs, with respectively the two legs in the same face and the leg in the external face:

$$\begin{aligned} R_0 &= R \frac{x + \frac{1}{x} + 1}{x + \frac{1}{x} + 2} = R - g^2 R^4 \\ S_0 &= S - gR^2 \end{aligned} \quad (6.21)$$

In particular, R_0 is the generating function for rooted trivalent planar graphs.

6.5. Arbitrary valences

The case of arbitrary valences still awaits a good solution, in the same spirit as the case of even valences. It is however possible to find “integrable-like” solutions to the corresponding recursion relations (containing only one integration constant), which for the time being are still too restrictive to describe the general case. Indeed, we need a sufficient number of integration constants to allow for satisfying all the necessary initial conditions of our combinatorial problem. This number is exactly the degree of the characteristic equation of the linearized recursions, when expressed as a polynomial in $x + 1/x$.

For arbitrary values of g_3, g_4, g_5, \dots we have the following “one- x ” solutions:

$$\begin{aligned} R_n &= R \frac{(1 - \lambda x^{n+1})(1 - \lambda x^{n+3})}{(1 - \lambda x^{n+2})^2} \\ S_n &= S - \sqrt{Rx} \frac{(1 - x)^2 \lambda x^n}{(1 - \lambda x^{n+1})(1 - \lambda x^{n+2})} \end{aligned} \quad (6.22)$$

where x is any solution with modulus less than 1 to the corresponding linearized characteristic equation. The latter reads for instance in the case of tri/tetravalent graphs where only g_3 and g_4 are non-zero:

$$\left(g_4 R \left(x + \frac{1}{x} + 4 \right) + S(2g_3 + 3g_4 S) - 1 \right)^2 - R(g_3 + 3g_4 S)^2 \left(x + \frac{1}{x} + 2 \right) = 0 \quad (6.23)$$

and amounts to

$$\sqrt{R}(g_3 + 3g_4S)(\sqrt{x} + \frac{1}{\sqrt{x}}) = 1 - g_4R(x + \frac{1}{x} + 4) - S(2g_3 + 3g_4S) \quad (6.24)$$

as R has a power series expansion of the form $R = 1 + O(g_3, g_4)$. In this particular case, it would be desirable to obtain the full solution involving the two roots x_1 and x_2 of (6.23) and two integration constants, to be able to solve simultaneously the two boundary conditions $R_{-1} = 0$ and $R_{-1}S_{-1} = 0$ (to be understood as $\lim_{n \rightarrow -1} R_n S_n = 0$) obtained from (5.9) at $n = 0$, and clearly not satisfied by (6.22).

6.6. Bipartite p -valent case

Repeating the usual exercise with eq.(5.13) in which we first eliminate X_n , we have found the following solution, including only one integration constant:

$$R_n = R \frac{u_n u_{n+p+1}}{u_{n+1} u_{n+p}}, \quad u_n = 1 - \lambda x^{n+1} \quad (6.25)$$

valid provided x is chosen among the roots of modulus less than 1 of the linearized characteristic equation:

$$1 - g\tilde{g}_1 R^{p-2} \frac{1}{x^{p-2}} (1 + x + x^2 + \dots + x^{p-2})^2 = 0 \quad (6.26)$$

As noticed in the case of planar graphs of arbitrary valences, the degree of this polynomial of $x + 1/x$ is however $p - 2$, hence only for $p = 3$ is the solution (6.25) completely general. This is the case of bipartite trivalent planar graphs, for which eq.(5.13) reduces to $R_n = 1 + g\tilde{g}_1 R_n (R_{n+1} + R_{n-1})$. In this case, the solution is further fixed by requiring $R_{-1} = 0$, hence $\lambda = 1$, and it reads

$$R_n = R \frac{(1 - x^{n+1})(1 - x^{n+5})}{(1 - x^{n+2})(1 - x^{n+4})} \quad (6.27)$$

with $1 - g\tilde{g}_1 R(x + 1/x + 2) = 0$, $|x| < 1$. R_n is the generating function for bipartite trivalent graphs with two legs attached to vertices of opposite colors, and geodesic distance between those less or equal to n . In particular,

$$R_0 = R \frac{x^2 + \frac{1}{x^2} + x + \frac{1}{x} + 1}{(x + \frac{1}{x})(x + \frac{1}{x} + 2)} = R \frac{1 - 3g\tilde{g}_1 R + g^2 \tilde{g}_1^2 R^2}{1 - 2g\tilde{g}_1 R} \quad (6.28)$$

is the generating function for rooted bipartite trivalent planar graphs (with weights g/\tilde{g}_1 per black/white vertex)

For $p \geq 4$, we must work out the generalizations of (6.10), which now read as follows. Introducing

$$\begin{aligned} p(x) &= x(1 + x + \dots + x^{p-2}), & q(x) &= p(1/x) \\ p_i &= p(x_i), & q_i &= q(x_i) \\ c_{i,j} &= \frac{(p_i - p_j)(q_i - q_j)}{(p_i - q_j)(q_i - p_j)} \end{aligned} \quad (6.29)$$

where x_i , $i = 1, 2, \dots, p-2$ denote the generically distinct roots of eq.(6.26) with modulus less than 1, the general solution now takes the form

$$R_n = R \frac{u_n^{(m)} u_{n+p+1}^{(m)}}{u_{n+1}^{(m)} u_{n+p}^{(m)}} \quad (6.30)$$

with $m = p-2$ and as before

$$u_n^{(m)} = \sum_{l=0}^m (-1)^l \sum_{1 \leq i_1 < i_2 < \dots < i_l \leq m} \prod_{t=1}^l \lambda_{i_t} x_{i_t}^n \prod_{1 \leq r < s \leq l} c_{i_r, i_s} \quad (6.31)$$

Note the absolutely remarkable fact that we obtain again an expression in terms of the tau-function for the KP hierarchy, but with different kinematics, in the form of an implicit relation between the p 's and q 's of eq.(6.29).

Imposing moreover the vanishing of the first terms $u_{-1} = u_{-2} = \dots = u_{-p+1}$, we find that

$$\lambda_i = x_i^{(p-1)m-1} \prod_{j \neq i} \frac{q_i - p_j}{p_i - p_j} \quad (6.32)$$

This fixes completely the solution to our combinatorial problem, and in particular gives a compact expression for the generating function R_0 for rooted bipartite p -valent planar graphs. For $p = 4$ for instance, it reads

$$R_0 = R \frac{1 - 5g\tilde{g}_1 R^2 + 3g^2 \tilde{g}_1^2 R^4}{1 - 3g\tilde{g}_1 R^2} \quad (6.33)$$

while R satisfies $R = 1 + 3g\tilde{g}_1 R^3$.

6.7. Constellations

The solution for general p -constellations is similar to that for pure p -valent bipartite graphs. Indeed, we find that the general solution has the exact same form (6.30) as in the previous section, with $u_n^{(m)}$ given by (6.31) and $p_i, q_i, c_{i,j}$ defined as in (6.29). The only

difference is that now m may take a larger value say $(p-1)k-1$ in the case when only $g, \tilde{g}_1, \tilde{g}_2, \dots, \tilde{g}_k$ are non-zero (namely of constellations with white p valent vertices, and black vertices with valences $p, 2p, \dots, kp$). The x 's entering these formulas are now the generically distinct roots with modulus less than 1 of the linearized characteristic equation, itself a polynomial of degree $(p-1)k-1$ of $x+1/x$, reading

$$1 = \left(1 + \frac{1}{x} + \dots + \frac{1}{x^{p-2}}\right) \sum_{i \geq 1} g^i \tilde{g}_i R^{(p-1)i-2} \sum_{m=0}^{(p-1)i-1} \sum_{j=0}^{i-1} \binom{j+m}{m} \binom{pi-2-j-m}{i-j-1} x^{m-j(p-1)} \quad (6.34)$$

For illustration, in the case of 3-constellations with say only g and \tilde{g}_2 non-zero (R_n obeys eq.(5.12) with $\tilde{g}_1 = 0$), we get the linearized characteristic equation:

$$1 - g^2 \tilde{g}_2 R^3 \left(x + \frac{1}{x} + 2\right) \left(x^2 + \frac{1}{x^2} + x + \frac{1}{x} + 6\right) = 0 \quad (6.35)$$

of degree 3 in $x+1/x$. Picking the three roots with $|x_i| < 1$, we finally get the generating function for rooted 3-constellations with white trivalent and black hexavalent vertices

$$R_0 = R \frac{1 - 17g^2 \tilde{g}_2 R^3 + 25g^4 \tilde{g}_2^2 R^6}{1 - 10g^2 \tilde{g}_2 R^3} \quad (6.36)$$

while R satisfies the equation (4.5) with only g and \tilde{g}_2 non-zero, namely $R = 1 + 10g\tilde{g}_2 R^4$.

6.8. Ising model

We have not been able to find a nice structure for the general solution of the even-valent bipartite case in general. In the particular case of the Ising model with zero magnetic field (eq.(5.17)), we have been able to derive all possible solutions involving only one integration constant.

The usual linearization of eq.(5.17) yields the following characteristic equation

$$\left(x + \frac{1}{x} + \frac{c}{gV(1-3gV)} - \frac{1-gV}{gV}\right) \left(x + \frac{1}{x} - \frac{c}{gV(1-3gV)} - \frac{1-gV}{gV}\right) \times \left(x + \frac{1}{x} + \frac{1+gV}{gV}\right) = 0 \quad (6.37)$$

of degree 3 in $x+1/x$. As already discussed before, we would need in principle to find the full solution to (5.17) that converges at large n , including all three x_1, x_2, x_3 , respectively the roots of the three factors in eq.(6.37) with modulus less than 1, and therefore including

also three integration constants. We now display the solutions with one x for each of the three factors in (6.37).

For both $x = x_1$ and $x = x_2$, we have found that

$$V_n = V \frac{u_n u_{n+3}}{u_{n+1} u_{n+2}}, \quad u_n = 1 - \lambda x^n \quad (6.38)$$

while for $x = x_1$:

$$R_n = R - V \frac{\lambda(1-x)(1-x^2)x^n}{u_{n+1}u_{n+2}} \quad (6.39)$$

and for $x = x_2$:

$$R_n = R + V \frac{\lambda(1-x)(1-x^2)x^n}{u_{n+1}u_{n+2}} \quad (6.40)$$

For $x = x_3$ however, the solution is quite different:

$$\begin{aligned} V_n &= V \frac{u_n u_{n+3}}{u_{n+1} u_{n+2}} \\ u_n &= 1 - 2\lambda x^n - z\lambda^2 x^{2n} \\ z &= \frac{((c-2)(x + \frac{1}{x}) + c - 8)((c+2)(x + \frac{1}{x}) + c + 8)}{(x^2 + \frac{1}{x^2} - (c-4)(x + \frac{1}{x}) - (c-2))(x^2 + \frac{1}{x^2} + (c+4)(x + \frac{1}{x}) + (c+2))} \end{aligned} \quad (6.41)$$

The growing complexity of the solutions lets us expect a quite involved general three x -solution, yet to be found.

7. Continuum limit

The exact solutions of Sect. 6 allow us to investigate the properties of the corresponding classes of planar graphs in terms of the geodesic distance, in the limit when the latter becomes large. This limit must clearly be taken simultaneously with the so-called critical limit of large graphs, reached in turn by letting the various weights per vertex approach some critical locus, corresponding to approaching the finite radii of convergence of the various combinatorial series involved.

The large n limit of $R_n = R + a_1 x_1^n + \dots$ where x_1 is the largest root with modulus less than 1 of the characteristic equation, leads to the natural definition of a correlation length $\xi = -\text{Log}|x_1|$, governing the exponential decay of $R_n - R \sim \exp(-n/\xi)$ as a function of the geodesic distance n . A good continuum limit may therefore be reached by letting x_1 (and possibly other x 's) tend to the value 1, while simultaneously keeping n/ξ , the continuum geodesic distance, fixed. This in turn implies certain relations between the vertex weights are reached, via the characteristic equation relating them to the x 's. These relations express nothing but the abovementioned critical limit, which must therefore be taken simultaneously with the continuum one.

7.1. Tetravalent case

We illustrate the above with the case of tetravalent graphs, with R_n given by (6.7). The critical limit $g \rightarrow g_c = 1/12$ is reached by taking say

$$g = g_c(1 - \epsilon^4), \quad R = \frac{R_c}{1 + \epsilon^2} \quad (7.1)$$

with $R_c = 2$, and the solution of eq.(6.2) with modulus less than 1 reads

$$x(g) = \frac{1 + 2\epsilon^2 - \epsilon\sqrt{3(2 + \epsilon^2)}}{1 - \epsilon^2} \quad (7.2)$$

hence $x = e^{\epsilon\sqrt{6}} + O(\epsilon^2)$ as $\epsilon \rightarrow 0$, and $\xi \propto 1/\epsilon$. Finally setting

$$n = \frac{r}{\epsilon} \quad (7.3)$$

we may simply express the continuum limit of the quantity R_n , or more interestingly that of $R - R_n$, generating two-leg diagrams of tetravalent planar graphs with distance at least n between the two legs. We find that

$$\mathcal{F}(r) = \lim_{\epsilon \rightarrow 0} \frac{R - R_n}{\epsilon^2 R} = \frac{3}{\sinh^2\left(\sqrt{\frac{3}{2}}r\right)} \quad (7.4)$$

This is the continuum two-point correlation function for random surfaces with two marked points at (rescaled) geodesic distance larger or equal to r . It coincides with the scaling function derived in [17], by use of transfer matrix formalism. This in turn yields the continuum two-point correlation function for random surfaces with two marked points at (rescaled) geodesic distance r :

$$\mathcal{G}(r) = -\mathcal{F}'(r) = 3\sqrt{6} \frac{\cosh\left(\sqrt{\frac{3}{2}}r\right)}{\sinh^3\left(\sqrt{\frac{3}{2}}r\right)} \quad (7.5)$$

This result may in turn be interpreted in terms of graphs with large but finite number N of vertices. Indeed, the above scaling relations (7.1) and (7.3) imply the following relation between the correlation length and the deviation from the critical point $\xi \sim (g_c - g)^{-\nu}$, with the exponent $\nu = 1/4$, and therefore the fractal dimension $d_F = 1/\nu = 4$ for the present model of random planar surfaces. More concretely, this tells us in particular that the number of faces in a large graph lying at geodesic distance $\leq n$ from the external

one behaves as $n^{d_F} = n^4$. A simple measure of this number is indeed the ratio $R_n|_{g^N}/R_0|_{g^N}$ of the corresponding coefficients of g^N in the two power series expansions, giving the proportion of graphs with the two legs distant by at most n to that with the two legs in the same face. Using our exact solution and performing a saddle-point expansion, we find

$$\lim_{N \rightarrow \infty} \frac{R_n|_{g^N}}{R_0|_{g^N}} \sim \frac{3}{56} n^4 \quad (7.6)$$

giving an explicit illustration of the fractal dimension 4.

This suggests to set $n = rN^{1/4}$ and to write $R_n|_{g^N}$, again by use of a saddle-point expansion, as

$$R_n|_{g^N} \sim \frac{4}{\pi} \frac{(12)^N}{N^{3/2}} \int_0^\infty duu^2 \left(1 + \operatorname{Re} \mathcal{F}(r\sqrt{-iu}) \right) \quad (7.7)$$

and similarly for $R|_{g^N}$ with \mathcal{F} replaced by 0. The ratio $R_n|_{g^N}/R|_{g^N}$ gives the probability $P(r)$ for a random surface with two marked points that their geodesic distance be less or equal to r :

$$P(r) = \frac{2}{\sqrt{\pi}} \int_0^\infty duu^2 e^{-u^2} \left(1 + \operatorname{Re} \mathcal{F}(r\sqrt{-iu}) \right) \quad (7.8)$$

7.2. Arbitrary even valences, multicriticality

Repeating the analysis of previous section for the case of graphs with even valences say up to $2m+2$, various critical points may be reached in the space of weights g_j . Concretely, picking the particular weights that ensure the following form for (2.3):

$$\frac{g_c - g}{g_c} = \left(\frac{V_c - V}{V_c} \right)^{m+1} \quad (7.9)$$

where $V = gR$, $g_4 = g$, $g_{2j} = g^j z_j$ fixed by the form (7.9) and $V_c = m/6$, $g_c = m/(6(m+1))$, the corresponding multicritical limit is obtained by setting

$$g = g_c(1 - \epsilon^{2(m+1)}), \quad R = R_c \frac{1 - \epsilon^2}{1 - \epsilon^{2(m+1)}} \quad (7.10)$$

with $R_c = V_c/g_c = m+1$. Remarkably, the characteristic equation (6.9) then turns into

$$\chi_m(x) = \left(\frac{V_c - V}{V_c} \right)^m P_m \left(\frac{1 - \epsilon^2}{\epsilon^2} \left(x + \frac{1}{x} - 2 \right) \right) = 0 \quad (7.11)$$

for some fixed degree m polynomial

$$P_m(u) = \sum_{l=0}^m (-u)^l \frac{l!}{(2l+1)!} \frac{m!}{(m-l)!} \quad (7.12)$$

This allows to get the leading behavior of the various x 's as

$$x_i = e^{-a_i \epsilon} + O(\epsilon^2) \quad (7.13)$$

where a_i^2 are the roots of P_m , and a_i are taken with positive real part. Consequently all the x 's tend to 1 simultaneously, and the correlation length of the problem reads $\xi \sim 1/\epsilon$, hence we now have the relation $\xi \sim (g_c - g)^{-\nu}$ with $\nu = 2(m + 1)$, i.e. a fractal dimension $d_F = 2(m + 1)$.

The multicritical continuum limit is therefore still obtained by setting (7.3), and the exact solution (6.10) yields the following two-point correlation of random surfaces with multicritical weights (known to simulate non-unitary matter conformal field theories with central charges $c(2, 2m + 1) = 1 - 3(2m - 1)^2 / (2m + 1)$ coupled to two-dimensional quantum gravity), with two marked points at geodesic distance less or equal to r :

$$\mathcal{F}(r) = -2 \frac{d^2}{dr^2} \text{Log } \mathcal{W} \left(\sinh \left(a_1 \frac{r}{2} \right), \sinh \left(a_2 \frac{r}{2} \right), \dots, \sinh \left(a_m \frac{r}{2} \right) \right) \quad (7.14)$$

where $\mathcal{W}(f_1, f_2, \dots, f_m)$ stands for the Wronskian determinant $\det [f_i^{(j-1)}]_{1 \leq i, j \leq m}$.

It is known from matrix model solutions that the general case of arbitrary valences leads to the same multicritical points. In particular we expect the scaling functions (7.14) to be the same at these points. The same remark applies to constellations as well. New multicritical points corresponding to conformal theories with central charges $c(p, q) = 1 - 6(p - q)^2 / (pq)$ for p, q two coprime integers can be reached within the framework of two-matrix models, corresponding to the general bipartite graphs. In the latter case, we expect some new scaling functions, characteristic of these other universality classes. An example will be given in next section, when discussing the Ising model.

7.3. Critical/continuum limit in general

The (multi-) critical continuum limits are reached by letting a number of the roots x of the characteristic equation tend to 1 simultaneously.

An alternative route for deriving the critical continuum limit of say the tetravalent case would have been to postulate the form $R_n = R(1 - \epsilon^2 \mathcal{F}(n\epsilon))$ and plug this ansatz into the recursion relation (5.1). With $g = g_c(1 - \epsilon^4)$, expanding the equation up to order 4 in ϵ , we arrive at the following differential equation for \mathcal{F} :

$$\mathcal{F}''(r) - 3\mathcal{F}^2(r) - 6\mathcal{F}(r) = 0 \quad (7.15)$$

The function \mathcal{F} of eq.(7.4) is the unique solution to (7.15) such that $\mathcal{F}(0) = \infty$ and $\mathcal{F}(\infty) = 0$.

More generally, we may derive differential equations for the multicritical cases of Sect.7.2 as well. These take the form

$$\mathcal{R}_{m+1}[1 + \mathcal{F}] = \mathcal{R}_{m+1}[1] \quad (7.16)$$

where $\mathcal{R}_m[u]$ is the m th KdV residue $(d^2 - u)^{m-1/2}|_{d^{-1}}$ where $d \equiv d/dr$ [20]. For instance, in the case of multicritical tetra/hexavalent graphs ($m = 2$) eq.(7.16) reads

$$\mathcal{F}^{(4)}(r) - 10\mathcal{F}(r)\mathcal{F}''(r) - 10\mathcal{F}''(r) - 5(\mathcal{F}'(r))^2 + 10(\mathcal{F}(r))^3 + 30(\mathcal{F}(r))^2 + 30\mathcal{F}(r) = 0 \quad (7.17)$$

Even more generally, recall that the KdV residues naturally arise (e.g. in the context of matrix model solutions) when solving the differential operator equation $[P, Q] = 1$, where $Q = d^2 - u$ and P some degree $2m + 1$ differential operator. The equation indeed boils down to $2d/dr(\mathcal{R}_{m+1}[u]) = 1$. In the present case, we rather have to write the equation $[P, Q] = 0$, which turns into $\mathcal{R}_{m+1}[u] = \text{const}$.

At the discrete level, comparing say (5.1) with the equations determining the matrix model solution for tetravalent graphs of arbitrary genus, we simply would have to replace 1 by n/N in the r.h.s. of (5.1). We may think of the differential operator $Q = d^2 - u$ as the continuum limit of the operator Q (5.2) defined in Sect.5.2, now acting on functions of the variable $r = n\epsilon$. In the other cases described in Sect.6, we always have such an operator Q at hand and again the recursion relations resemble strongly those obtained in the solutions of the multi-matrix models describing two-dimensional quantum gravity coupled with matter, up to the same substitution $1 \rightarrow n/N$. This suggests that the relevant (coupled) differential equations governing the (multi-) critical continuum limit should read $[P, Q] = 0$, with Q the continuum limit of the operator say Q_1 used in our approach, taking the form of a differential operator of degree q say, and P a differential operator of degree p coprime with q . Our claim is that the generalized two-point functions $\mathcal{F}(\nabla)$ for random surfaces in the presence of critical matter (corresponding to conformal field theories with central charges $c(p, q) < 1$), with two marked points at geodesic distance less than r , should be governed by $[P, Q] = 0$, where $Q = d^q - qu d^{q-2} \dots$, and $u = 1 + \mathcal{F}$. This is illustrated in the case of the Ising model in the next section.

7.4. Ising model

The multicritical limit of the Ising model is obtained as follows. Starting from the equations (4.9) rewritten as $W(R) = 0$, W a polynomial of degree 5, the tri-critical points are determined by setting $W'(R) = W''(R) = 0$, and we find that $c_c = \pm 4$ while $g_c = 10/9$, and $R_c = -3/5$, $V_c = -3/10$. The tricritical limit is approached by setting

$$c = 4, \quad R = R_c(1 - \epsilon^2) \quad \Rightarrow \quad g = g_c(1 - \frac{16}{5}\epsilon^6) \quad (7.18)$$

We note that in the characteristic equation (6.37) only the first and last factor tend to $x + 1/x - 2$ as $\epsilon \rightarrow 0$, while the middle one tends to $x + 1/x + 10$. This means that only two of the three x 's tend to 1 in this limit. More precisely, we have $x_3 = e^{-\sqrt{6}\epsilon} + O(\epsilon^2)$ and $x_1 = e^{-2\sqrt{3}\epsilon} + O(\epsilon^2)$. This displays the fractal dimension of graphs with critical Ising configurations, namely $d_F = 6$, obtained by expressing the correlation length $\xi \sim (g_c - g)^{-\nu}$, where $\nu = 1/6$. Recall however that the distance n or its rescaled version r are slightly different from the true geodesic distance in the Ising tetravalent graphs, and the fractal dimension measured here might be different from that associated to the true geodesic distance.

Further substituting

$$\begin{aligned} R_n &= R(1 - \epsilon^2 \mathcal{F}(n\epsilon)), & r &= n\epsilon \\ V_n &= \frac{R_n}{c + g(R_{n+1} + R_n + R_{n-1})} \end{aligned} \quad (7.19)$$

into the recursion relations (5.17) together with (7.18), we find by expanding up to order 6 in ϵ that the two-point function \mathcal{F} obeys the differential equation

$$\mathcal{F}^{(4)}(r) - 18\mathcal{F}(r)\mathcal{F}''(r) - 18\mathcal{F}''(r) - 9(\mathcal{F}'(r))^2 + 24(\mathcal{F}(r))^3 + 72(\mathcal{F}(r))^2 + 72\mathcal{F}(r) = 0 \quad (7.20)$$

This equation is precisely what one would get by writing $[P, Q] = 0$ for differential operators $Q = d^3 - 3ud - 3u'/2$ and P of order 4, $u = 1 + \mathcal{F}$.

Looking for convergent solutions in the form $\mathcal{F}(r) = ae^{-kr}$, we find that $k_1 = \sqrt{6}$ or $k_2 = 2\sqrt{3}$, corresponding to $e^{-k_1 r} = x_3^n$ and $e^{-k_2 r} = x_1^n$ respectively. Proceeding like in the discrete case, we may now solve the differential equation order by order in $e^{-k_i r}$, with a double power series expansion $\mathcal{F}(r) = \sum_{m,p \geq 0} a_{m,p} e^{-r(mk_1 + pk_2)}$, in terms of the two integration constants $\lambda = a_{1,0}$, $\mu = a_{0,1}$, while $a_{0,0} = 0$. The differential equation (7.20)

indeed simply amounts to a recursion relation on the coefficients $a_{m,p}$. Resumming the series for $\mathcal{F}(r)$ finally yields:

$$\mathcal{F}(r) = -\frac{d^2}{dr^2} \text{Log} \left(1 - \frac{\lambda}{6} e^{-r\sqrt{6}} - \frac{\mu}{12} e^{-2r\sqrt{3}} - \frac{\lambda^2}{288} e^{-2r\sqrt{6}} - \frac{17 - 12\sqrt{2}}{72} \lambda \mu e^{-r(\sqrt{6}+2\sqrt{3})} + \frac{577 - 408\sqrt{2}}{3456} \lambda^2 \mu e^{-2r(\sqrt{6}+\sqrt{3})} \right) \quad (7.21)$$

The two integration constants are further fixed by the boundary conditions. The latter are obtained by requiring that the recursion relations (5.17) also make sense at $n = 0, 1$, namely $R_{-1} = V_{-1} = 0$, while $\lim_{n \rightarrow 0} V_{n-1} V_{n-2} = 0$. The first conditions give $\mathcal{F}(0) = \infty$, while the latter implies $R_{-1} R_{-2} = 0$. As in the case of planar graphs with only tetra/hexavalent vertices, this implies a higher order vanishing of the argument of the logarithm in (7.21), which plays the role of continuum limit of u_n , while the condition implies that both u_{-1} and u_{-2} vanish. This is easily solved into $\lambda = -12(17 + 12\sqrt{2})$ and $\mu = 12(4 + 3\sqrt{2})$, so that finally

$$\mathcal{F}(r) = -\frac{d^2}{dr^2} \text{Log} \left(\sinh(r(\sqrt{6}+\sqrt{3})) + (17+12\sqrt{2}) \sinh(r(\sqrt{6}-\sqrt{3})) - 2(4+3\sqrt{2}) \sinh(r\sqrt{3}) \right) \quad (7.22)$$

and we also get the correlation $\mathcal{G}(r) = -\mathcal{F}'(r)$ for the Ising model on random surfaces, with two marked points at (special) geodesic distance r .

8. Conclusion

In this note, we have addressed the problem of enumeration of various types of planar graphs with external legs, while keeping track of a suitable geodesic distance between these legs. The basic tool we used are blossom-trees, namely trees carrying the minimal information needed to close them back into planar graphs. This information is essentially contained in the two types of leaves (black and white), and we have devised a compact algebraic way of keeping track of the geodesic distance between legs, by introducing operators Q describing the structure of the rooted trees around their first vertex. This operator acts formally on a basis $|n\rangle$ indexed by relative integers, and may as well be viewed as acting on sequences $\{p_n\}_{n \in \mathbb{Z}}$, via the shift operator σ and its relative integer powers, and a number of (combinatorial) diagonal operators. This definition is clearly borrowed from that of the Q operator of matrix models, that generate the multiplication by an eigenvalue

λ on the basis of (right) monic (bi-)orthogonal polynomials $p_n(\lambda)$, $n = 0, 1, 2, \dots$. In this framework, the main recursion relations for the coefficients of Q are obtained by considering the operator P , acting on the $p_n(\lambda)$ by differentiation w.r.t. λ . The canonical relation $[P, Q] = 1$ determines in fact all the functions of the problem, and turns into differential equations in the critical scaling limit. Here, by analogy with this case, we have been led to set $[P, Q] = 0$, for some operator P still awaiting a good combinatorial meaning. Nevertheless, this equation also turns into differential equations for the physical quantities of our problem. The mysterious part of this correspondence is that the natural variable in the matrix model approach is the rescaled cosmological constant, which generates the topological expansion of the free energy, namely the expansion in powers of r of the function $u(r)$ has coefficients corresponding to planar graphs of fixed genus. This must be contrasted with the present findings, where r has the meaning of geodesic distance. This seems to indicate that a more general structure should exist, that includes both the topological and geodesic directions, probably some suitably defined matrix model of sorts.

In view of these strong analogies with matrix model solutions, we may want to characterize the class of possibly decorated planar graphs for which a tree formulation exists as that for which there exists a matrix model formulation admitting a solution via orthogonal polynomials. This would exclude for instance the case of the three-state Potts model, a generalization of the Ising model whose configurations are graphs with vertices of three possible colors, and edge weights $w_{a,b} = e^{K\delta_{a,b}}$ according to the colors a, b of the adjacent vertices. More generally, loop models on graphs also correspond to matrix models without orthogonal polynomial solutions: their configurations are simply mutually- and self-avoiding loops drawn on the edges of planar graphs, with a weight n per loop (the so-called $O(n)$ model, extensively solved in [21]). It would be extremely interesting to investigate any of these models using tree techniques.

A final striking outcome of our work is the emergence of soliton-like tau functions entering the explicit exact formulas for a number of generating functions for two-leg diagrams with legs distant by at most n . A reason why this should happen in the first place may be perhaps traced back to the integrability of the recursion relations we have obtained. A first indication of this integrability is the existence of “integrals of motion” for these equations. For instance, the recursion relation of the tetravalent case, eq.(5.1), has the following integral of motion:

$$\begin{aligned}
 f(R_n, R_{n+1}) &= \text{const.} \\
 f(x, y) &= xy(1 - gx - gy) - x - y
 \end{aligned}
 \tag{8.1}$$

as is immediately checked by forming

$$f(R_n, R_{n+1}) - f(R_n, R_{n-1}) = (R_{n+1} - R_{n-1})(R_n - 1 - gR_n(R_{n+1} + R_n + R_{n-1})) \quad (8.2)$$

More generally, one may construct such integrals of motion for all the models studied in this note. Again, it may be that this integrability property relates to the existence, for the same planar graphs but with arbitrary topology rather than planar with fixed geodesic distances, of matrix model formulations that are solvable via orthogonal polynomial techniques.

Acknowledgments This note summarizes work essentially done in collaboration with J. Bouttier and E. Guitter. We also thank M. Bousquet-Mélou and G. Schaeffer for fruitful discussions on constellations and bipartite graphs.

References

- [1] E. Brézin, C. Itzykson, G. Parisi and J.-B. Zuber, *Planar Diagrams*, Comm. Math. Phys. **59** (1978) 35-51.
- [2] P. Di Francesco, P. Ginsparg and J. Zinn-Justin, *2D Gravity and Random Matrices*, Physics Reports **254** (1995) 1-131.
- [3] B. Eynard, *Random Matrices*, Saclay Lecture Notes (2000), available at http://www-spht.cea.fr/lectures_notes.shtml
- [4] W. Tutte, *A Census of planar triangulations* Canad. Jour. of Math. **14** (1962) 21-38; *A Census of Hamiltonian polygons* Canad. Jour. of Math. **14** (1962) 402-417; *A Census of slicings* Canad. Jour. of Math. **14** (1962) 708-722; *A Census of Planar Maps*, Canad. Jour. of Math. **15** (1963) 249-271.
- [5] V.G. Knizhnik, A.M. Polyakov and A.B. Zamolodchikov, *Fractal Structure of 2D Quantum Gravity*, Mod. Phys. Lett. **A3** (1988) 819-826; F. David, *Conformal Field Theories Coupled to 2D Gravity in the Conformal Gauge*, Mod. Phys. Lett. **A3** (1988) 1651-1656; J. Distler and H. Kawai, *Conformal Field Theory and 2D Quantum Gravity*, Nucl. Phys. **B321** (1989) 509-527.
- [6] G. Schaeffer, *Bijective census and random generation of Eulerian planar maps*, Electronic Journal of Combinatorics, vol. **4** (1997) R20; see also G. Schaeffer, *Conjugaison d'arbres et cartes combinatoires aléatoires* PhD Thesis, Université Bordeaux I (1998).
- [7] J. Bouttier, P. Di Francesco and E. Guitter, *Census of planar maps: from the one-matrix model solution to a combinatorial proof*, Nucl. Phys. **B645**[PM] (2002) 477-499.
- [8] M. Bousquet-Mélou and G. Schaeffer, *Enumeration of planar constellations*, Adv. in Applied Math., **24** (2000) 337-368.
- [9] J. Bouttier, P. Di Francesco and E. Guitter, *Counting colored Random Triangulations*, Nucl.Phys. **B641** (2002) 519-532.
- [10] D. Poulalhon and G. Schaeffer, *A note on bipartite Eulerian planar maps*, preprint (2002), available at <http://www.loria.fr/~schaeffe/>
- [11] J. Bouttier, P. Di Francesco and E. Guitter, *Combinatorics of hard particles on planar maps*, Nucl. Phys. **B655** (2003) 313-341.
- [12] M. Bousquet-Mélou and G. Schaeffer, *The degree distribution in bipartite planar maps: application to the Ising model*, preprint math.CO/0211070.
- [13] P. Chassaing and G. Schaeffer, *Random Planar Lattices and Integrated SuperBrownian Excursion*, preprint (2002), to appear in Probability Theory and Related Fields, math.CO/0205226.
- [14] J. Bouttier, P. Di Francesco and E. Guitter, *Random trees between two walls: Exact partition function*, J. Bouttier, P. Di Francesco and E. Guitter, Saclay preprint t03/086 and cond-mat/0306602 (2003), to appear in J. Phys. A: Math. Gen. (2003).

- [15] J. Bouttier, P. Di Francesco and E. Guitter, *Geodesic distance in planar graphs*, Nucl. Phys. **B 663**[FS] (2003) 535-567.
- [16] H. Kawai, N. Kawamoto, T. Mogami and Y. Watabiki, *Transfer Matrix Formalism for Two-Dimensional Quantum Gravity and Fractal Structures of Space-time*, Phys. Lett. B **306** (1993) 19-26.
- [17] J. Ambjørn and Y. Watabiki, *Scaling in quantum gravity*, Nucl.Phys. **B445** (1995) 129-144.
- [18] J. Ambjørn, J. Jurkiewicz and Y. Watabiki, *On the fractal structure of two-dimensional quantum gravity*, Nucl.Phys. **B454** (1995) 313-342.
- [19] M. Jimbo and T. Miwa, *Solitons and infinite dimensional Lie algebras*, Publ. RIMS, Kyoto Univ. **19** No. 3 (1983) 943-1001, eq.(2.12).
- [20] I. Gelfand and L. Dikii, *Fractional powers of operators and Hamiltonian systems*, Funct. Anal. Appl. **10:4** (1976) 13.
- [21] B. Eynard and C. Kristjansen, *Exact Solution of the $O(n)$ Model on a Random Lattice*, Nucl.Phys. **B455** (1995) 577-618, and *More on the exact solution of the $O(n)$ model on a random lattice and an investigation of the case $|n| > 2$* , Nucl.Phys. **B466** (1996) 463-487.